NATIONAL ADVISORY COMMITTEE FOR AERONAUTICS

TECHNICAL NOTE 3393

AN EXPERIMENTAL INVESTIGATION OF THE BASE PRESSURE CHARACTERISTICS OF NONLIFTING BODIES OF REVOLUTION AT MACH NUMBERS FROM 2.73 TO 4.98

By John O. Reller, Jr., and Frank M. Hamaker

Ames Aeronautical Laboratory
Moffett Field, Calif.

Washington
March 1955

NATIONAL ADVISORY COMMITTEE FOR AERONAUTICS

TECHNICAL NOTE 3393

AN EXPERIMENTAL INVESTIGATION OF THE BASE PRESSURE CHARACTERISTICS OF NONLIFTING BODIES OF REVOLUTION AT MACH NUMBERS FROM 2.73 TO 4.98[1]

By John O. Reller, Jr., and Frank M. Hamaker

SUMMARY

An investigation was undertaken in the Ames 10- by 14-inch supersonic wind tunnel to determine some of the base pressure characteristics of related bodies of revolution at zero angle of attack. The basic body shape used in this investigation was a 10-caliber tangent ogive nose section combined with a cylindrical afterbody. Other related shapes tested differed in that they had either a blunt-nosed profile or a boattailed afterbody. Model fineness ratios were varied from 3.12 to 10 by changing afterbody length. Tests were conducted at free-stream Mach numbers from 2.73 to 4.98 over a Reynolds number range, based on body length, from 0.6×10^6 to 8.8×10^6.

In general, the base pressure coefficient decreased with increasing Reynolds number and increased with increasing free-stream Mach number and fineness ratio. In the particular case of an ogive-cylinder model of fineness ratio 5 with laminar-boundary-layer flow at a Reynolds number of 4×10^6, it was found that the base pressure coefficient was about 60 percent of the limiting value (represented by a vacuum) over the Mach number range of the tests. A decrease in the base pressure coefficient, which became more pronounced with increasing Mach number, accompanied natural transition from laminar- to turbulent-boundary-layer flow in the region of the base. This result is in contrast to that obtained at lower supersonic Mach numbers where an increase in base pressure coefficient has been found to accompany transition.

The effect on the measured base pressure of the nose-profile shapes investigated was found to be negligible for an afterbody length of 7 body diameters. With turbulent-boundary-layer flow over a body of fineness

[1]Supersedes recently declassified NACA RM A52E20 by John O. Reller, Jr., and Frank M. Hamaker, 1952.

ratio 7, the substitution of a 6-caliber ogival boattail (base diameter equals 0.604 maximum diameter) for the cylindrical afterbody resulted in an increase in the base pressure coefficient of approximately 75 percent at a Mach number of 1.50 (as determined from tests in the Ames 1- by 3-foot supersonic wind tunnel) but only about 22 percent at a Mach number of 4.48. Corresponding values for laminar flow were 36 and 28 percent, respectively.

INTRODUCTION

The pressure acting on the base of a body moving at supersonic speeds may be of considerable practical importance since it can produce base drag amounting to more than one-half of the total drag of the body. Early attempts to predict the base pressure on bodies of revolution in supersonic flow were made by Lorenz, Gabeaud, and von Kármán (see references 1, 2, and 3, respectively). It is now recognized, however, (see, e.g., reference 4) that these methods are generally inadequate because they do not account for effects of body shape on the inviscid flow in the region approaching the base nor do they account for the effects of viscosity. The more recent results of Hill (reference 5) are similar to those obtained in reference 3 and would appear to be unsatisfactory for these same reasons.

Semiempirical theories of base pressure for bodies of revolution have been developed by Cope (reference 6) and Chapman (reference 4). In contrast with the preceding investigations, these methods attempt to include not only the effects of Mach number but also the effects of viscosity by considering the influence of the boundary-layer flow in the region of the base. Cope's method is designed to predict base pressures, provided that, in addition to free-stream conditions, the thickness and type of the boundary layer at the base and the distance from the base to the trailing shock wave are known. Because of the numerous assumptions and approximations that are made in developing this method, however, it is, according to Cope, no more than a first approximation. The method provides only a qualitative prediction of the base pressures of bodies of revolution at low supersonic Mach numbers.

Chapman's method, on the other hand, is essentially a means of correlating experimental data at a given Mach number, and, as such, requires the use of fewer simplifying assumptions in its development. If the necessary experimental constants are known from a previous correlation, it has been found that the method can be used to predict, with reasonable accuracy, the base pressures for similar bodies of revolution at low supersonic airspeeds.

It is evident then, that at present an adequate knowledge of the base pressure phenomenon remains strongly dependent on results of experiments. A large amount of base pressure data are available from both wind-tunnel and free-flight tests at low supersonic airspeeds. At high supersonic speeds, however, only a limited amount of data are available, and the accuracy of the proposed methods of references 4 and 6 for either correlating or predicting base pressures has not been verified.

The primary purpose of this investigation is to determine experimentally the variation of base pressure with Reynolds number at high supersonic Mach numbers. To this end, several related, nonlifting bodies of revolution have been investigated at Mach numbers from 2.73 to 4.98 and Reynolds numbers (based on body length) varying from about 0.6×10^6 to 8.8×10^6 in the Ames 10- by 14-inch supersonic wind tunnel.

NOTATION

d	maximum model diameter
d_s	model support diameter
l	length of model
l_s	length of model support
M	Mach number
p	static pressure
P_b	base pressure coefficient referred to free-stream conditions $\left(\frac{p_b-p_o}{q_o}\right)$
P_{b_1}	base pressure coefficient referred to conditions just ahead of the base $\left(\frac{p_b-p_1}{q_1}\right)$
q	dynamic pressure $\left(\frac{1}{2}\rho U^2\right)$

r	local radius of body
Re	Reynolds number based on model length
U	resultant velocity
x	axial distance from the body vertex
γ	ratio of specific heat at constant pressure to specific heat at constant volume
ϵ	correction parameter, defined by equation (2)
ρ	density

Subscripts

a	stagnation conditions
b	conditions at base
o	conditions in free stream
1	conditions just ahead of base
2	conditions on surface of extended afterbody

APPARATUS AND TEST PROCEDURE

Wind-Tunnel and Auxiliary Equipment

This investigation was conducted in the Ames 10- by 14-inch supersonic wind tunnel. The tunnel is of the closed-throat, continuous-flow type and consists of a deLaval nozzle followed by a test section and a converging-diverging diffuser. Details of the wind tunnel can be found in reference 7. A simple shadowgraph system was employed to identify the type of boundary-layer flow. McLeod type gages, each of which was equipped with a trap containing dry ice and acetone to remove condensable vapors, were used to measure pressures.

Models

The majority of the bodies tested were ogive cylinders with 10-caliber tangent ogival noses and cylindrical afterbodies of 1-inch diameter; the over-all fineness ratios varied from 3.12 to 10 (see models 1 through 4, fig. 1(a)). A 1-1/2-inch-diameter model of fineness ratio 5 was also tested, primarily for the purpose of measuring the pressure distribution across the base. This model (model 5) and its special support are shown in figure 1(b).

A small amount of data was obtained with models that had noses of fineness ratio 3 defined by the equation $r = 0.219\,x^{3/4}$. (This shape is approximately that of a body for minimum drag for an l/d of 3, as pointed out in reference 7.) These noses were faired into 1-inch-diameter cylindrical afterbodies (see models 6 and 7 in fig. 1(c)). One additional ogive-cylinder model with a boattailed afterbody was also tested (see fig. 1(c) showing model 8; d = 1.25 in., base diameter = 0.604d). Data obtained on these models were used to evaluate some of the effects of nose and afterbody shape on base pressure.

Model number 2 ($l/d = 5$) was used with supports of various lengths and diameters (see fig. 2) to evaluate the effect of support interference on measured base pressure.

The quality of model surface finish may influence the measured base pressure through its effect on boundary-layer development. The test models had, therefore, a general surface finish of about 10 microinches (average deviation from the mean surface).

Test Procedure

Operating conditions.- For this investigation the wind tunnel was operated at Mach numbers from 2.73 to 4.98, with a maximum reservoir pressure of 6 atmospheres absolute and reservoir temperatures between 50° F and 70° F. The absolute humidity of the air supplied to the tunnel was maintained between 1.5×10^{-5} and 5.0×10^{-5} pounds of water per pound of air. The Reynolds number of the flow at Mach numbers of 2.73 and 4.98 was approximately 8.2×10^6 per foot and 2.1×10^6 per foot, respectively. At intermediate Mach numbers a range of Reynolds numbers was available with the maximum range of 3.6×10^6 to 8.6×10^6 per foot occurring at a Mach number of 4.03.

Methods of promoting a turbulent boundary layer.- In an attempt to extend the range of Reynolds numbers at which a turbulent boundary layer would occur, several types of turbulence-promoting devices were investigated. Tests were conducted with rings of 0.005- and 0.010-inch-diameter wire and salt bands of various widths, located both near the vertex and at the shoulder of a model. A lampblack coating on the nose of a model was also tried. Several of the turbulence-promoting devices are illustrated in figure 3. It was found that a salt band of approximately 0.020-inch thickness and 1/2-inch width, located 1/4 inch from the vertex of a model, was the only device that was effective in causing the boundary layer to become turbulent for the complete range of Mach numbers and Reynolds numbers of this investigation. With this device, the transition point was fixed at the location of the roughness. The salt-band roughness was therefore used as the turbulence-promoting device in the majority of tests. Some turbulent-boundary-layer data were obtained for model 8 with a 0.005-inch-diameter wire ring located close to the vertex. The effectiveness of this device in promoting turbulence was limited to the higher test Reynolds numbers at Mach numbers below 4.5.

INTERPRETATION AND REDUCTION OF THE DATA

Boundary-Layer Identification

A representative series of shadowgraph pictures for both laminar- and turburlent-boundary-layer flow is shown in figure 4. Laminar-boundary-layer flow is identified by the characteristic light line that is apparent near the model surface and that extends downstream from the base. Turbulent-boundary-layer flow, on the other hand, is identified by a diffused light region adjacent to the surface and a lack of detail in the expansion region behind the base. The type of boundary-layer flow is also indicated by the location of the trailing shock wave behind the model. For turbulent flow this shock wave stands closer to the base than for laminar flow at the same Mach number and Reynolds number.

It is necessary to specify the conditions under which the base pressure data of this report correspond to those for laminar-, transitional-, and turbulent-boundary-layer flow in the region of the base. The data correspond to laminar-boundary-layer flow when the laminar appearance of the flow (identified by the characteristic light line) persists downstream of the base to the location of the trailing shock wave. Similarly, in every case of turbulent-boundary-layer flow, transition started at least 3- to 4-base diameters upstream of the base. Data that were measured under conditions that fall between these two limits are considered to be representative of transitional-boundary-layer flow.

Support Interference

Models were supported in the wind tunnel by a cylindrical rod extending from the base. Since this configuration is significantly different from a body with an unobstructed base, the measured values of base pressure may be considerably altered. Tests were conducted over the entire Mach number and Reynolds number range to determine the extent of the influence of both support length and support diameter on the base pressure. Typical results are shown in figures 5 and 6. On the basis of these results it seems reasonable to assume that with a d_s/d ratio of 0.40 or less and an l_s/d ratio of 8, the measured base pressure is essentially free of support interference. Because of the varying loads encountered in the base pressure tests, it was necessary to use d_s/d ratios as great as 0.625 and l_s/d ratios as low as 6. Therefore it was often necessary to apply corrections, based on the results of this investigation, to the measured base pressure coefficients that are presented in the following discussion. The effects of support interference and the correction method are considered in more detail in appendix A.

Condensation in the Air Stream

As a result of the large flow expansion that takes place in the nozzle of a high supersonic-speed wind tunnel, extremely low static temperatures are realized in the flow passing through the test section. At a settling chamber temperature of about 60° F, the existing situation in the Ames 10- by 14-inch supersonic wind tunnel, the static temperature in the free stream falls below the liquefaction temperature at Mach numbers somewhat in excess of 4.0. Consequently, as has been shown in reference 8, at these Mach numbers a portion of the air in the wind tunnel will enter the condensed phase and thus the properties of the stream will be altered. As discussed in appendix B, this phenomenon affects both the boundary-layer flow and the flow field outside of the boundary layer. It is shown in appendix B that, for the purposes of these tests, these influences on the boundary layer can be neglected, but that the alteration of the expansion process in the flow downstream of the base may increase the base pressure coefficient by as much as 12 percent at the highest test Mach number. (This corresponds to an increase in the base pressure relative to the free-stream static pressure.) Since the method used to evaluate this effect of condensation is only approximate, the basic data of the present report are presented both as corrected and uncorrected for condensation effects.

Effect of Transition-Promoting Device

To obtain turbulent boundary layers on a representative number of models at several Reynolds numbers, it was necessary, as previously discussed, to locate a transition-promoting device close to the vertex of each model. However, this device caused a systematic change in the base pressures. This fact is demonstrated for models 4 and 5 in figure 7 where a comparison is made of the base pressures obtained with natural transition to a turbulent boundary layer with those obtained with fixed transition to a turbulent boundary layer resulting from the use of the artificial roughness. It can be seen that the base pressure coefficient measured with fixed transition was from about 7 to 11 percent higher. Shadowgraph pictures showed, correspondingly, an increase in boundary-layer thickness which, it is believed, would account for the greatest percentage of the observed difference. This difference in base pressure coefficient, in other words, is attributed primarily to effects of the artificial roughness on the turbulent boundary layer rather than to effects of the artificial roughness on the flow field outside the boundary layer. In certain qualitative respects the use of an artificial transition-promoting device would appear to be analogous, then, to testing with a model of greater length on which the turbulent boundary layer had developed to a greater thickness. At present, however, insufficient data are available to permit a general correction to be made for this effect. Thus, although the relative variations of the base pressure coefficient with Reynolds number and Mach number for the turbulent boundary layer with fixed transition are believed representative, the actual values of base pressure coefficient are probably high by as much as 10 percent. Unless specifically stated otherwise, all base pressure data with turbulent-boundary-layer flow that are subsequently presented in this report were obtained with the use of a transition-promoting device.

PRECISION OF THE DATA

Pressure Measurement

The operational plus the reading error of the McLeod pressure gages varied from ±2-1/2 percent to ±1/2 percent at the lowest and highest measured pressures, respectively. The rate of leakage into the pressure-measuring systems introduced an uncertainty of less than 1/2 percent. Reservoir pressure was determined to within ±1-percent accuracy, while free-stream static and dynamic pressures were obtained from wind-tunnel calibration data which are also accurate to within ±1 percent at all test Mach numbers.

Pressure Gradients in the Test Section

The free-stream static and dynamic pressures used in the reduction of these data are those which exist on the center line of the wind tunnel (tunnel empty) in the plane of the base of the test model. Since the vertices of all models were located at the same station in the test section, the position of the plane of the base of the different models varied as much as 7 inches along the axis. Within this distance, the maximum variation of Mach number is ±1.2 percent of the mean value (see reference 7). Maximum errors in base pressure coefficient less than ±2 percent are therefore introduced by relating these data to the effective test Mach number. At Mach number 4.48, a weak pressure discontinuity intersected the axis close enough to the base of the longest model to influence the base pressure. The error from this source was estimated to cause an increase in P_b of less than 3 percent.

Summation of Errors

The various sources of uncertainty in the measured base pressures and the corresponding maximum and probable errors that could be introduced into the absolute values of the base pressure coefficients are listed in the following table. The maximum error would result if all possible errors that are known to exist were to accumulate. The probable error, that is the root-mean-square value of the errors from the several sources, would more nearly result if, as is usually the case, the errors were partially compensating.

	Error in P_b at $M_o = 2.73$	Error in P_b at $M_o = 4.98$
Pressure measurement	±3 percent	±4-1/2 percent
Pressure gradient in test section	±2 percent	±2 percent
Maximum error	±5 percent	±6-1/2 percent
Probable error	±3-1/2 percent	±5 percent

RESULTS AND DISCUSSION

Variation of Pressure Over the Base

The results of the investigation to determine the variation of pressure over the base of a body of revolution at high supersonic Mach numbers are shown in figure 8. Base pressures on model 5 were measured on the model support at the base of the model as well as along two radial lines on the base, one in the horizontal plane and the other in the vertical plane of the wind tunnel. Although pressures were determined over a range of Reynolds numbers at each Mach number, only representative data are presented. In general, it is observed that changes in pressure coefficient with radial location are small. The differences, at the lower Mach numbers, between pressures in the vertical and horizontal planes are attributed to pressure gradients in the tunnel air stream in the corresponding directions normal to the tunnel center line. These differences are increased in the case of turbulent flow due to a partial deterioration of the artificial roughness that was not discovered until completion of the tests. It is noted that in all cases, however, these differences are small, and that the pressure measured on the model support represents a reasonably good average value. The base pressure data to be discussed subsequently were therefore obtained at this location.

Variation of Base Pressure With Reynolds Number

Constant body fineness ratio.- Base pressure coefficients for the $l/d = 5$, ogive-cylinder combination are presented as a function of Reynolds number in figure 9 for laminar-boundary-layer flow. These coefficients, uncorrected for condensation in the expansion region downstream of the model, are shown in figure 9(a), while those corrected for condensation by the approximate method discussed in appendix B are shown in figure 9(b).[2] As would be expected, the base pressure coefficient decreases (corresponding to decreasing base pressure relative to free-stream pressure) with increasing Reynolds number. It is clear that in general, however, the effect of Reynolds number on the coefficient decreases as the free-stream Mach number increases. For example, at $M_o = 3.49$ an increase of Reynolds number from 3×10^6 to 4.5×10^6 changes the coefficient about 20 percent, while at $M_o = 4.48$ a similar increase of Reynolds number results in a change of only about 5 percent.

[2]It will be noted that the trends and relative magnitudes of the corrected data are essentially the same as those for the uncorrected data. This property is characteristic of all data to be presented; hence the discussion of results may generally be considered to apply to both types of data.

Data are presented in figure 10 for turbulent-boundary-layer flow. It can be seen that the variation of pressure coefficient with Reynolds number is similar for all Mach numbers above 2.73. It is also evident from a comparison with figure 9 that the effect of Reynolds number is somewhat less at lower Mach numbers than for the laminar boundary layer, which agrees with the results of other investigators. However, at $M_0 = 4.48$ and 4.98, the converse is true as seen in figures 9 and 10. At a Mach number of 2.73 the base pressure coefficient increases slightly with increasing Reynolds number. A similar effect has been observed at $M_0 = 1.5$ and 2.0 with turbulent-boundary-layer flow and reported in reference 4.

Influence of body fineness ratio.- Base pressure coefficients for ogive-cylinder models of fineness ratios 3.12 to 10 are presented as a function of Reynolds number in figure 11 for laminar-boundary-layer flow. It can be seen that the variations of pressure coefficient with Reynolds number, for a given Mach number, are generally similar for the different l/d ratios tested. As would be expected, the base pressure coefficient at a constant Reynolds number and Mach number increases with increasing body fineness ratio. This variation can be attributed, in part, to the increase in pressure recovery on the cylindrical afterbody just ahead of the base, with increasing fineness ratio. However, it may also be attributed in part to the increase in boundary-layer thickness at the base (d = const.) with increasing fineness ratio.

Similar data are presented in figure 12 for turbulent-boundary-layer flow. Again it can be seen that the variation with Reynolds number (at a constant M_0) is similar for the l/d ratios tested, and that the base pressure coefficient (at constant Re and M_0) increases with increasing fineness ratio as for the case previously discussed. A correlation of these data by the method of reference 4 is presented in a later section.

Boundary-layer transition.- The variation of base pressure coefficient with Reynolds number for laminar-, transitional-, and turbulent-boundary-layer flow for the fineness ratio 5 ogive-cylinder models (models 2 and 5) is presented in figure 13. The data in the low Reynolds number range were obtained from figure 9, while the dashed lines in the high Reynolds number range were obtained by extrapolation from the curves of figure 10.[3] Also shown in figure 13 are the data of figure 7, at Mach number 3.49, for fully developed turbulent-boundary-layer flow resulting from natural boundary-layer transition. The onset of transition, that is, those conditions for which the transition point in the boundary-layer flow first moves to a position upstream of the trailing shock wave, was found in these tests to occur at Reynolds numbers between approximately 4×10^6 and 5×10^6.

[3]It will be recalled that the data of figure 10 were obtained with fixed transition resulting from the use of an artificial roughness.

It can be seen that a decrease of base pressure coefficient occurs in the Reynolds number range of transition at Mach numbers above 2.73. This effect becomes more pronounced as the Mach number increases, varying from approximately 15 percent (turbulent flow with fixed transition as compared to laminar flow) at $M_o = 3.49$ to 50 percent at $M_o = 4.48$. The change of base pressure coefficient with natural boundary-layer transition appears to be even larger. For example, at $M_o = 3.49$ the decrease is approximately 26 percent. From the previous discussion of the effect on base pressure coefficient of the transition-promoting device, it follows that the difference between turbulent flow with fixed and natural transition would be of similar magnitude at the other test Mach numbers. Thus, with natural boundary-layer development it appears that a decrease of base pressure coefficient occurs with transition for the entire Mach number range of the present tests. In contrast with these results, comparative data at $M_o = 1.5$ and $M_o = 2.0$ for a 20° cone-cylinder model of $l/d = 5$, taken from reference 4, show an increase in base pressure coefficient in the Reynolds number range of transition.[4] The reasons for this change of base pressure behavior with increasing Mach number are at present not completely understood; a partial verification of the phenomenon, however, is obtained from a consideration of the physical characteristics of the flow pattern downstream of the base. In particular, a difference in the location of the trailing shock wave, relative to the base, with laminar- as compared to turbulent-boundary-layer flow (at the same M_o and Re) is shown in the shadowgraph pictures of the present tests. In every case (see, e.g., fig. 4) the trailing shock wave stands closer to the base for turbulent flow than for laminar, with the difference increasing as the Mach number is increased. In general, then, it would be expected that for the turbulent case a greater flow expansion occurs around the corner of the base and thus a lower pressure is transmitted into the dead-air region. On the other hand, photographs at $M_o = 1.5$ (see fig. 21 of reference 9) for a similar ogive-cylinder body indicate that the shock wave stands somewhat closer to the base for laminar than for turbulent flow. General agreement is thus apparent between these limited observations and the trends shown in figure 13 of the present report.

Effect of Nose and Afterbody Shapes

For the study of nose-shape effects, base pressure data were obtained with models having ogival noses and the slightly blunt noses for minimum pressure drag (given l/d) at high supersonic airspeeds. The base pressure coefficients obtained with both laminar- and turbulent-boundary-layer flow in the region of the bases of these bodies are presented in figure 14.[5]

[4]Although this body shape is not identical to the $l/d = 5$ model used in the present tests, the indicated variations of the base pressure coefficient with Reynolds number are representative of the established trends at low supersonic Mach numbers.

[5]Only data corrected for condensation are presented in this and subsequent figures. Uncorrected data are related to these data in the manner discussed previously.

It is seen that base pressure coefficients with laminar flow (fig. 14(a)) for the blunt-nosed body of $l/d = 3.12$ are about 4 percent less than those for the corresponding ogival-nosed body at Mach numbers from 2.7 to 5.0 and a constant Reynolds number of 2.5×10^6. With turbulent-boundary-layer flow (fig. 14(b)), a similar result is observed for these bodies; for example, the base pressure coefficients for the blunt-nosed body vary from 7 percent less to about 3 percent less than those for the corresponding ogive as the Mach number increases from 2.7 to 4.5. It is seen, on the other hand, that when a cylindrical afterbody is added to these bodies to increase their over-all l/d to 10, no measurable effect of nose shape on base pressure coefficient is observed. That there is a reduction in this effect is not surprising, since it would be expected that with increasing afterbody length flow conditions in the region of the base (both within and outside the boundary layer) would become less sensitive to nose shape. It is interesting to note, however, that with the two different noses employed, the effect is essentially zero for an afterbody length of only 7 diameters.

Effects of boattailing were studied with model 8. A comparison of the base pressure coefficients for this body and the coefficients for the corresponding unboattailed body is shown in figure 15.[6] Also shown in figure 15 are data obtained with similar models in the Ames 1- by 3-foot supersonic wind tunnel at $M_0 = 1.5$ and 2.0. Some of these data are unpublished; the remainder are interpolated from data of references 4, 9, and 10. It is evident that the boattailed body consistently has the higher base pressures at Mach numbers from 1.5 to 4.5 for both laminar- and turbulent-boundary-layer flow in the region of the base. The effect of this amount of boattailing is observed to decrease markedly, however, with increasing Mach number. For example, in the case of turbulent-boundary-layer flow (see fig. 15(b)) boattailing increases the base pressure coefficient by 75 percent at $M_0 = 1.5$, while at $M_0 = 4.5$ it increases the coefficient by only 22 percent; corresponding values for laminar-boundary-layer flow are 36 percent and 28 percent, respectively. The results of reference 11, at a Mach number of 3.25, are in substantial agreement with those of figure 15.

Variation of Base Pressure with Mach Number

Base pressure coefficients for a body of fineness ratio 5 (model 2) with both laminar-boundary-layer flow and artificially induced turbulent-boundary-layer flow are presented as a function of free-stream Mach number in figure 16. The results were obtained from a cross plot of the data in figures 9 and 10. The limiting curve of base pressure coefficient (i.e., for a vacuum at the base) is shown for comparison. For the Mach number

[6]Results presented here were determined from cross plots of the data in figures 11 and 12 and similar figures for the boattailed body. Where necessary, the base pressure coefficient for model 3 was obtained by linear interpolation from the data of models 1, 2, and 4.

range of the present tests, it can be seen that the base pressure coefficient for laminar flow is about 60 percent of the limiting value. With an artificially induced turbulent boundary layer, the coefficient is smaller, increasing from about 62 percent to 82 percent of the limiting value as the Mach number is increased from 2.73 to 4.48. It is also interesting to note from a comparison of the high Mach number data of the present tests and the low Mach number results as interpolated from data of reference 4 that the same base pressure coefficients would apparently be obtained with both laminar-boundary-layer flow and artificially induced turbulent-boundary-layer flow at a Mach number of about 2.5. With natural transition to turbulent-boundary-layer flow, this Mach number would probably be slightly less. These results are, of course, consistent with those discussed previously in connection with figure 13.

The ratio of base pressure to free-stream static pressure is plotted as a function of free-stream Mach number in figure 17. The base pressure data are the same as those shown in figure 16, but are replotted in this form to expand the scale of the variation in the high Mach number range where the base pressure coefficient decreases to small magnitude. The base pressure ratio for laminar-boundary-layer flow remains relatively constant throughout the Mach number range of the present tests, in contrast with the trend indicated at lower supersonic Mach numbers by the data of reference 4. With turbulent flow the base pressure ratio decreases markedly up to $M_0 = 4$, but relatively slowly thereafter.

With regard to these indicated trends, the semiempirical method of Cope (reference 6) yields results that are in only qualitative agreement with the laminar base pressure curve of figure 17. For turbulent-boundary-layer flow this method fails to predict the observed variation of base pressure with free-stream Mach number; in fact, values similar to those for laminar flow were obtained. As a result, the intersection of the laminar and turbulent curves that would be indicated in figures 16 and 17 is not apparent from the analysis of reference 6.

Correlation of Base Pressure Data

A method of correlating base pressure data has been suggested by Chapman in reference 4. It is assumed in the correlation that the base pressure is primarily dependent upon the conditions just upstream of the base. Therefore, the measured base pressure coefficient P_b, which is referred to free-stream conditions, must be related to the coefficient P_{b_1} based on conditions just ahead of the base. The relationship between P_b and P_{b_1} is given in reference 4 as:

$$P_b = P_{b_1}(1+\epsilon) + P_2 \qquad (1)$$

$$\epsilon = \left(\frac{M_o^2}{2} - 1\right)P_2 - \frac{2}{\gamma M_o^2}\left(1 + \frac{\gamma-1}{2} M_o^2\right)\frac{\Delta p_a}{p_a} \qquad (2)$$

and Δp_a is the loss in total pressure through the nose shock wave. The parameter P_2 is considered to be a correction to P_b for the effects of profile shape and, as used herein, is defined as the pressure coefficient $(p_2-p_o)/q_o$ which would exist on the surface of a hypothetical cylindrical extension of the body at a point midway between the actual base and trailing shock wave.

In equation (1), P_{b_1} is considered to be independent of body shape for a given Mach number approaching the base. Since this Mach number varies somewhat for different l/d ratios, an additional correction, $\frac{\partial P_b}{\partial M}(M_1-M_o)$, to P_{b_1} is necessary to enable a direct comparison to be made between various body shapes (see reference 4). The resultant equation

$$P_{b_1} = \frac{P_b-P_2}{1+\epsilon} + \frac{\partial P_b}{\partial M}(M_1-M_o) \qquad (3)$$

was then used in the present correlation. Numerical values of the pressure coefficient P_2 were taken from reference 12. The values of P_{b_1} obtained from this equation were, as suggested in reference 4, correlated by plotting them as a function of the parameters $l/(d\sqrt{Re})$ and $l/[d(Re)^{1/5}]$, which are approximately proportional to boundary-layer thickness for laminar- and turbulent-boundary-layer flow, respectively.

The data of figures 11 and 12 are presented in this form in figure 18. For comparison, similar curves from reference 4 at Mach numbers 1.53 and 2.00 are also shown. For both laminar- and turbulent-boundary-layer flow, the variation of P_{b_1} with the boundary-layer parameters at each of the higher Mach numbers cannot, in contrast with the low Mach number data of reference 4, be completely represented by the single mean curve that is shown. In fact, for the present range of variables, it is apparent that the parameters do not bring the data for different fineness ratios into agreement. At a constant value of Mach number and fineness ratio, a large part of the higher Mach number data indicate, as shown by the short dashed lines in figure 18, a local slope that is appreciably greater than the slope of the mean curve. Thus on the basis of the experimental evidence available here, the usefulness of the method of base pressure correlation of reference 4 appears to be diminished at Mach numbers in excess of about 3.

CONCLUSIONS

A wind-tunnel investigation was conducted to determine some of the base pressure characteristics of several related bodies of revolution at zero angle of attack and free-stream Mach numbers from 2.73 to 4.98. In general, it was found that the base pressure coefficient increased with increasing free-stream Mach number and body fineness ratio and decreased with increasing Reynolds number, with either laminar- or turbulent-boundary-layer flow.

The following specific conclusions are drawn from the results of this investigation:

1. The base pressure coefficient is higher with laminar- than with turbulent-boundary-layer flow at Mach numbers above approximately 2.5.

2. A decrease of the base pressure coefficient occurs with natural transition from laminar- to turbulent-boundary-layer flow at Reynolds numbers from 4.0×10^6 to 6.0×10^6; this effect becomes more pronounced with increasing Mach number. At $M_o = 3.49$ on a body of fineness ratio 5 the decrease was approximately 26 percent.

3. With laminar-boundary-layer flow the variation of the base pressure coefficient with Reynolds number becomes less pronounced as the Mach number is increased.

4. A change of afterbody from a cylindrical shape to one with boattailing causes an increase in the base pressure coefficient. For turbulent-boundary-layer flow over a body with a 6-caliber ogival boattail (base diameter equals 0.604 maximum diameter) this effect decreased markedly with increasing Mach number from 75 percent at $M_o = 1.5$ to 22 percent at $M_o = 4.48$.

5. For an afterbody length of about 7 body diameters, the effect of nose profile shape on base pressure was found to be negligible for the nose shapes tested.

6. The semiempirical method of Cope is inadequate for predicting base pressures in the Mach number range of these tests, while the corresponding method of Chapman provides at most only an approximate correlation of experimental data at Mach numbers above about 3.

Ames Aeronautical Laboratory
National Advisory Committee for Aeronautics
Moffett Field, Calif., May 20, 1952

APPENDIX A

SUPPORT INTERFERENCE

The effects on base pressure of both support length and diameter were investigated over the entire Mach number and Reynolds number range, using model 2. Typical effects of support length for a constant diameter ($d_s/d = 0.375$) are illustrated in figure 5.[1] With a laminar boundary layer little change in base pressure coefficient is indicated from $M_o = 2.73$ to $M_o = 4.48$ for an unobstructed support length greater than 4 base diameters. At $M_o = 4.98$, however, this coefficient is significantly altered for support lengths less than 6 base diameters, and may be slightly altered for support lengths up to 8 diameters. With turbulent-boundary-layer flow there is no appreciable change in the base pressure coefficient for support lengths greater than 4 base diameters over the range of Mach numbers. A comparison is made in figure 5 with similar data at $M_o = 2.90$ from reference 4.

Typical variations of base pressure coefficient with support diameter are presented in figure 6. A constant support length-to-base-diameter ratio of 6 was used. With a laminar boundary layer at test Mach numbers above 2.73 there is no significant change in base pressure coefficient for support-to-base-diameter ratios less than 0.40. At $M_o = 2.73$, however, support interference persists to the lowest d_s/d ratio tested, although the effect is relatively small at d_s/d ratios below 0.40. On the basis of these results, it seems reasonable to assume that no significant variation of base pressure coefficient for laminar-boundary-layer flow will occur at d_s/d ratios between 0.40 and 0. For turbulent-boundary-layer flow at $M_o = 4.03$ and 4.48 there is a negligible change of the coefficient for support-to-base-diameter ratios less than 0.50. At the remaining Mach numbers the base pressure coefficient varies to some extent over the entire range of diameter ratios tested. However, at $M_o = 3.49$ and 4.98 this variation is small, indicating, for example, that P_b is approaching a limiting value in the former case for d_s/d ratios less than 0.40. (Comparable data from reference 4 are observed to show a similar trend of P_b with the ratio d_s/d at a Mach number of 2.90.) In general, then, it seems reasonable to assume that with turbulent-boundary-layer flow at Mach numbers above about 3.0, little change of the base pressure coefficient occurs at d_s/d ratios between 0.40 and 0. At $M_o = 2.73$ the variation of P_b with the d_s/d ratio does not approach a limiting value; however, the free-flight

[1]The data in this and the subsequent figure are not corrected for condensation, since trends only are discussed and absolute values are not essential.

data from reference 13[2] and the data from reference 4 shown in figure 6(b) indicate that the values of P_b at d_s/d from 0.25 to 0.375 do not differ appreciably from that at d_s/d of 0.

In view of the results of this support-interference investigation, support lengths of at least 6 base diameters were used in all subsequent tests. Support diameters were held to a minimum consistent with strength requirements, with d_s/d varying from 0.375 to 0.625 for the shortest and longest models tested, respectively. Measured base pressure coefficients were adjusted, using data represented by figures 5 and 6, to an l_s/d ratio of 8 and a d_s/d ratio of 0.375 to obtain data that are assumed to be essentially free of support interference effects.

No evaluation was made of the effects of support interference on the measured base pressures of the boattailed model. However, since a support with $l_s/d = 13$ was used, the data presented in figure 5 indicate that these base pressures are free of support-length interference. An investigation of support dimensions for a boattail model of similar shape with laminar-boundary-layer flow (reference 9) showed that at $M_o = 1.5$ interference effects are negligible with a support of approximately the same relative diameter ($d_s/d = 0.35$) as that used but of shorter relative length ($l_s/d = 7$). It is thus indicated, in view of the results presented in figure 6, that these pressures are also relatively free of support-diameter effects.

[2]The free-flight body of reference 13 was a 20° cone-cylinder combination of $l/d = 5$ instead of an ogive cylinder, but calculations show that the conditions on the model surfaces near the base are such that the base pressures of the two models should be closely comparable.

APPENDIX B

CONDENSATION IN THE AIR STREAM

An investigation of the condensation of air in supersonic flow has been reported in reference 8. It was shown experimentally that condensation occurs at free-stream Mach numbers above 4.4 in the Ames 10- by 14-inch supersonic wind tunnel. Therefore, the relationships given in appendix C of the reference report (applying when the air stream contains a small amount of condensed air) were used to determine the effective test Mach numbers 4.48 and 4.98 of the present report. The methods of reference 8 were also used to evaluate the effect of condensation upon the measured data of the present report. It was shown therein that the properties of the flow approaching the base of a body of revolution (outside the boundary layer) are approximately those that would exist at the same Mach number in a stream that was free of condensation. It was also shown that re-evaporation of the condensed phase occurs in the high temperature boundary-layer region of a test model. This may reduce the surface temperature by as much as 30° F ($M_o = 4.98$). Reference 11 indicates, however, that a surface temperature change of this magnitude will alter the base pressure by only about 1.5 percent. As a first approximation, therefore, the effects of condensation on the flow approaching the base, both inside and outside the boundary layer, may be considered negligibly small.

Condensation phenomena can, however, have an appreciable effect on flow in the expansion region downstream of the base. The amount of condensation that exists in this region can exceed that of the free stream as a result of the relatively high local Mach numbers and hence low static temperatures which occur. A static pressure rise is associated, of course, with this increased condensation and, in all likelihood, will be transmitted through the adjacent dead-air space to the base. An estimate of this rise in pressure was obtained graphically from a diagram similar to that shown in figure 3 of reference 8, in combination with calculated flow conditions approaching the base and the measured base pressures. One simplifying assumption was made; namely, that the process of condensation does not require an appreciable time interval or, in other words, that saturation or subsaturation conditions exist at every point in the flow. Based on this analysis, condensation effects on base pressure were found to occur at free-stream Mach numbers as low as 3.49. As would be expected, the maximum pressure rise occurred at the highest test Mach number, causing a change of about 12 percent in the measured base pressure coefficient. In view of the appreciable magnitude of this pressure change, it was considered desirable to present not only measured base pressure data but also the data corrected for the pressure rise. This is done throughout much of the present report and, although the correction is approximate, it may be looked upon as a maximum correction, inasmuch as saturation flow conditions were assumed.

REFERENCES

1. Lorenz, H.: Der Geschosswiderstand. Physikalische Zeitschrift, vol. 18, 1917, p. 209; vol. 29, 1928, p. 437.

2. Gabeaud: Base Pressures at Supersonic Velocities. Jour. Aero. Sci., vol. 16, no. 10, Oct. 1949, p. 638.

3. von Kármán, Th., and Moore, N. B.: The Resistance of Slender Bodies Moving at Supersonic Velocities. Trans. of ASME, vol. 54, 1932, pp. 303-310.

4. Chapman, Dean R.: An Analysis of Base Pressure at Supersonic Velocities and Comparison with Experiment. NACA TN 2137, 1950.

5. Hill, Freeman K.: Base Pressures at Supersonic Velocities. Jour. Aero. Sci., vol. 17, no. 3, Mar. 1950, pp. 185-187.

6. Cope, W. F.: The Effect of Reynolds Number on the Base Pressure of Projectiles. NPL Eng. Div. 63/44, Jan. 1945.

7. Eggers, A. J., Jr., Dennis, David H., and Resnikoff, Meyer M.: Bodies of Revolution for Minimum Drag at High Supersonic Airspeeds. NACA RM A51K27, 1952.

8. Hansen, C. Frederick, and Nothwang, George J.: Condensation of Air in Supersonic Wind Tunnels and Its Effects on Flow About Models. NACA TN 2690, 1952.

9. Chapman, Dean R., and Perkins, Edward W.: Experimental Investigation of the Effects of Viscosity on the Drag and Base Pressure of Bodies of Revolution at a Mach Number of 1.5. NACA Rep. 1036, 1951. (Formerly NACA RM A7A31a)

10. Perkins, Edward W.: Experimental Investigation of the Effects of Support Interference on the Drag of Bodies of Revolution at a Mach Number of 1.5. NACA TN 2292, 1951.

11. Kurzweg, H. H.: The Base Pressure Measurements of Heated, Cooled, and Boat-Tailed Models at Mach Numbers 1.5 to 5.0. Proceedings of the Bureau of Ordnance Symposium on Aeroballistics, NAVORD Rep. 1651, Nov. 16-17, 1950, pp. 119-142.

12. Rossow, Vernon J.: Applicability of the Hypersonic Similarity Rule to Pressure Distributions Which Include the Effects of Rotation for Bodies of Revolution at Zero Angle of Attack. NACA TN 2399, 1951.

13. Charters, A. C., and Turetsky, R. A.: Determination of Base Pressure from Free-Flight Data. Aberdeen Ballistic Res. Lab. Rep. No. 653, Mar. 30, 1948.

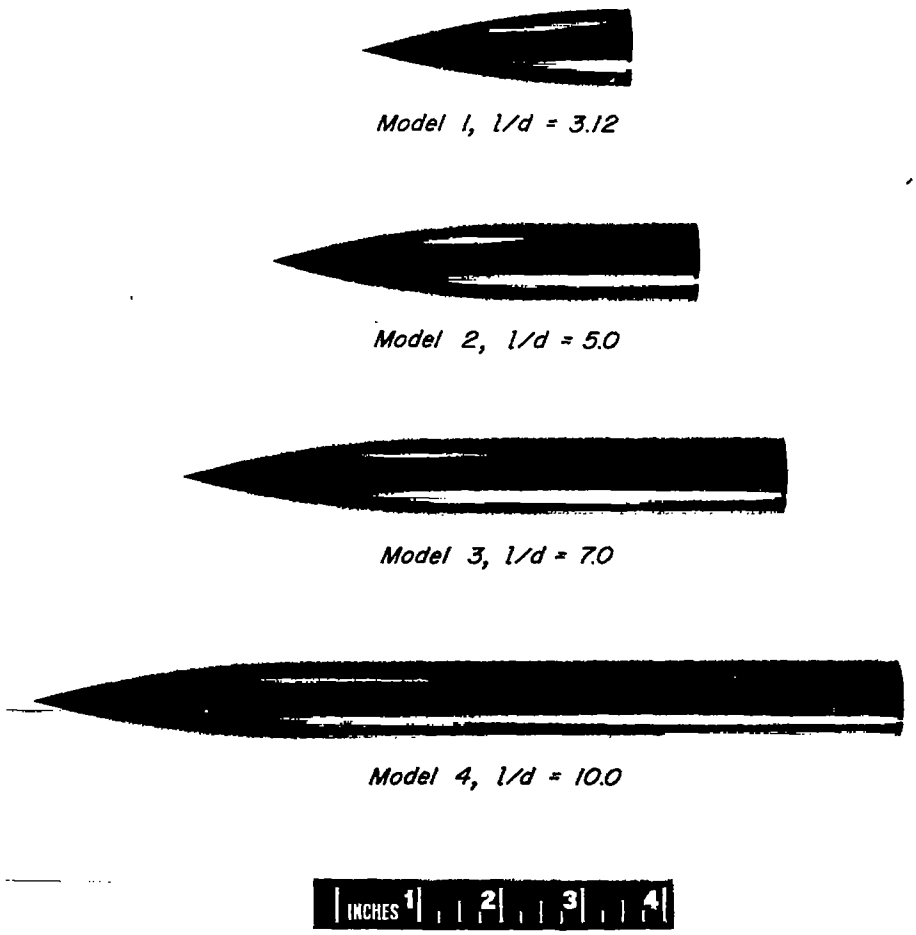

(a) Ogive–cylinder models.

Figure 1.– Models used in base pressure investigation.

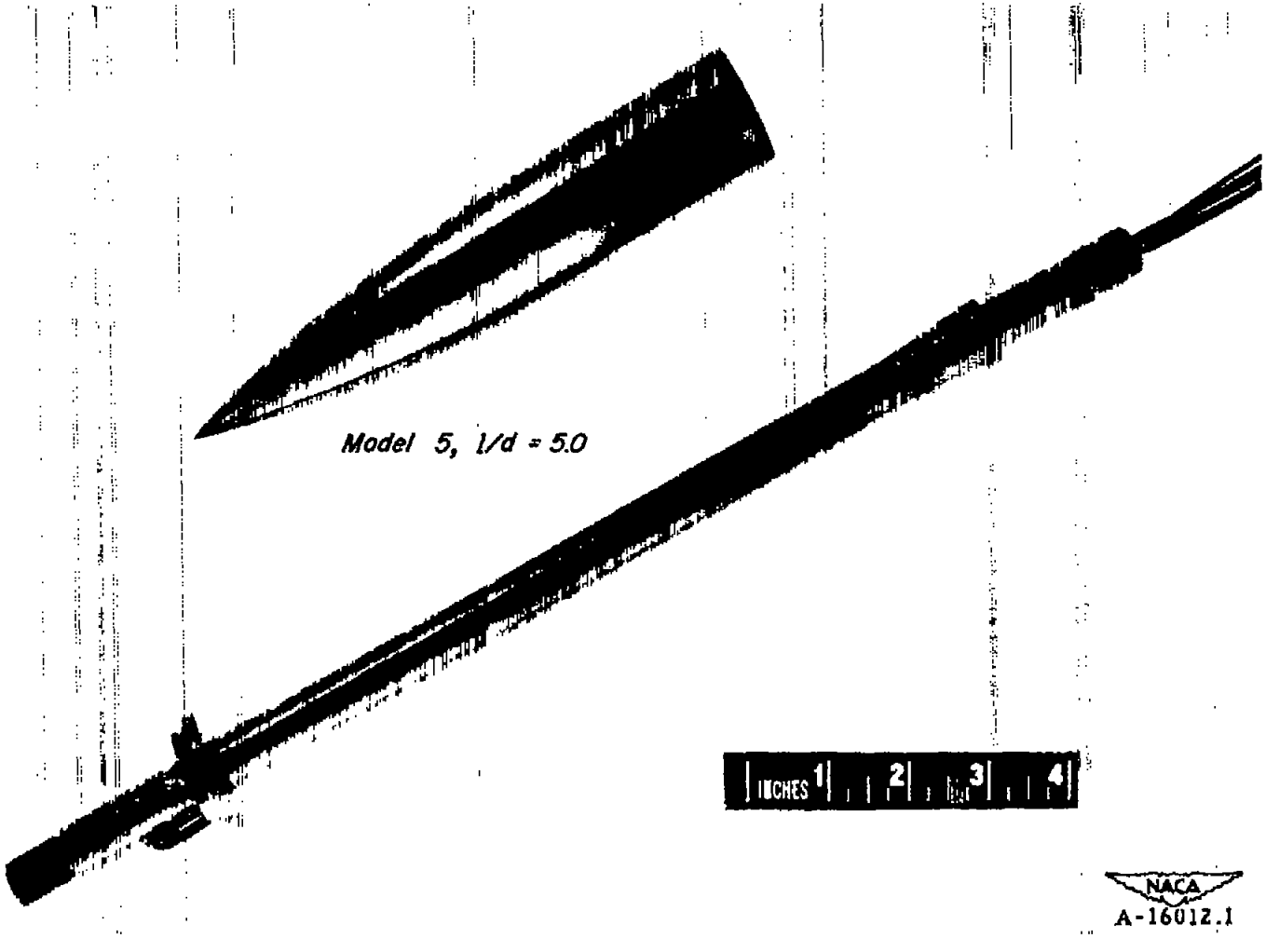

(b) Pressure gradient model and support.

Figure 1.– Continued.

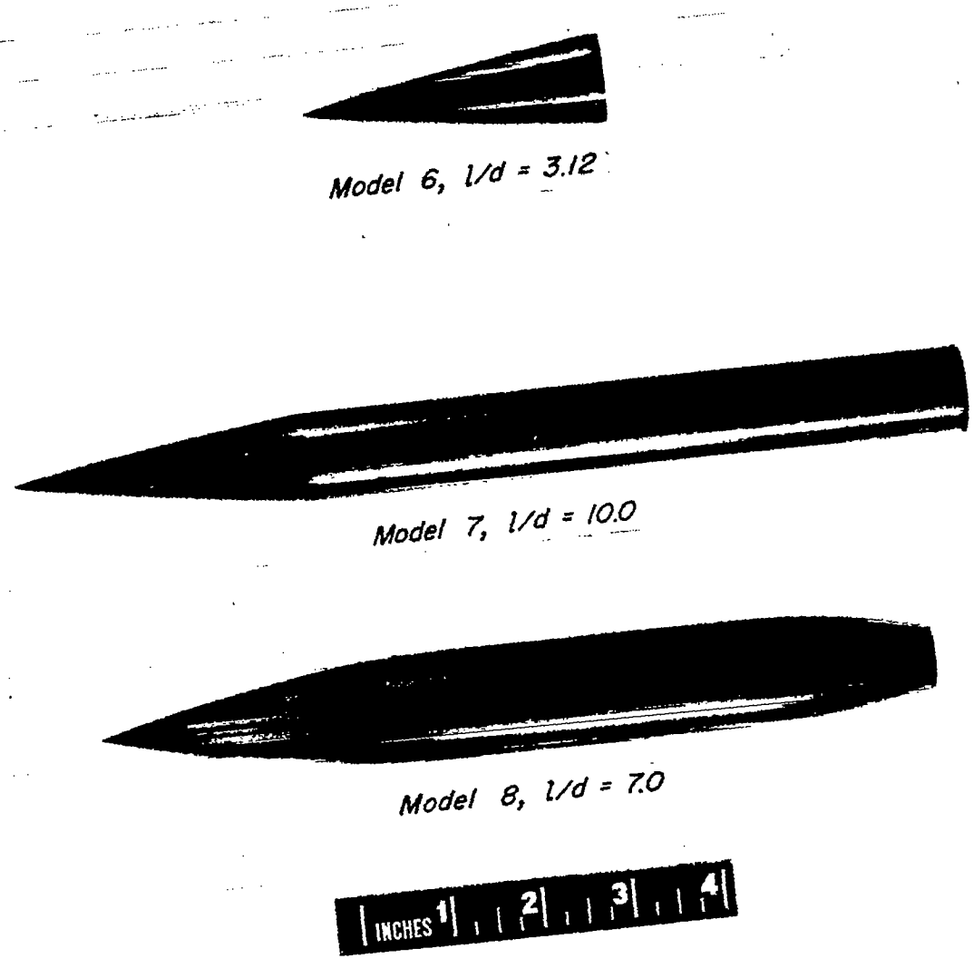

(c) Models used to study effects of nose shape and boattailing.

Figure 1.- Concluded.

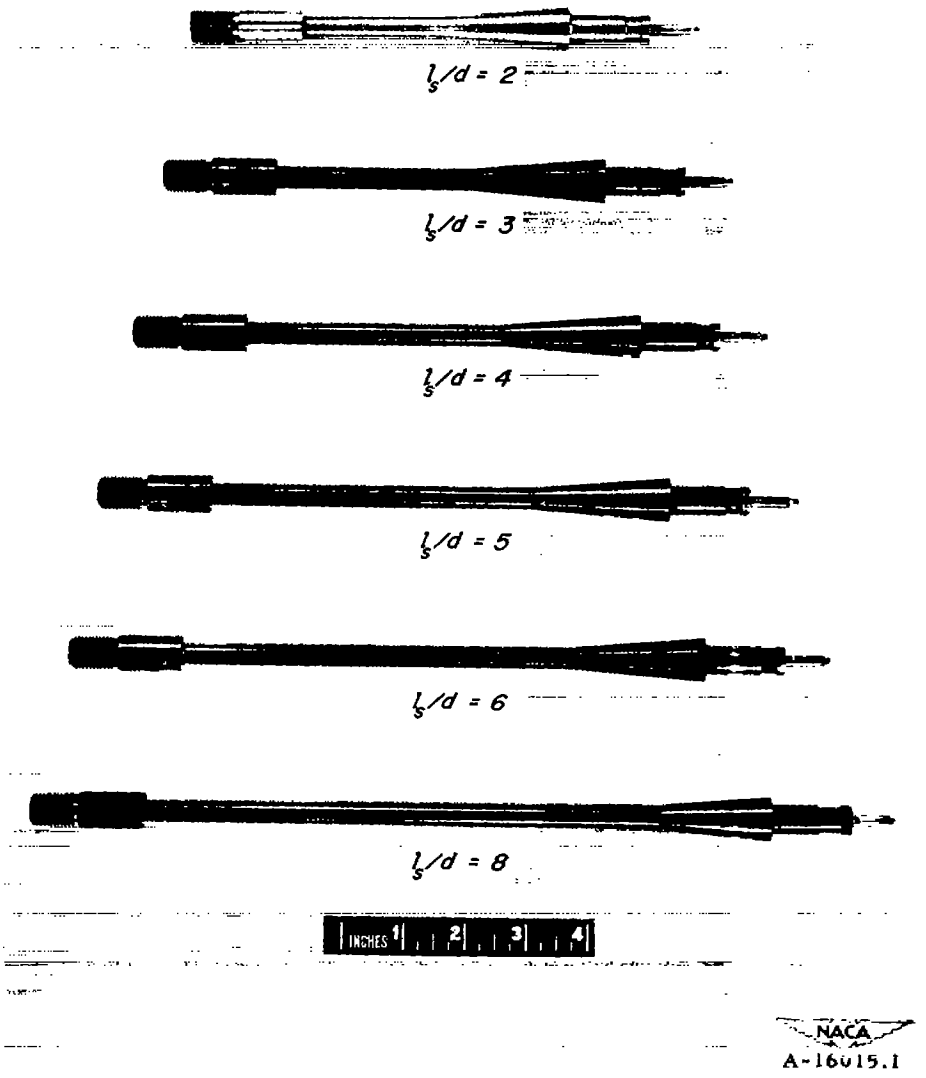

(a) Supports of various lengths, $d_s/d = 0.375$.

Figure 2.— Model supports used to study effect of support interference.

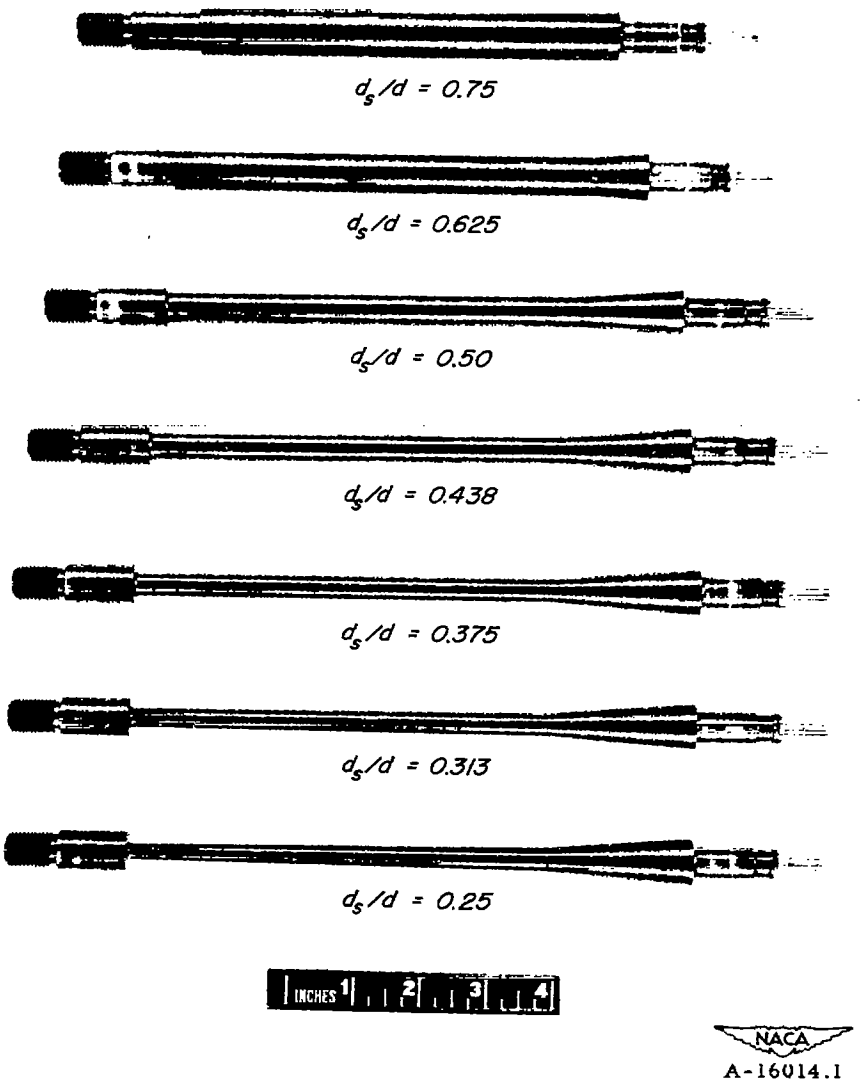

(b) Supports of various diameters, l_s/d = 6.0.

Figure 2.— Concluded.

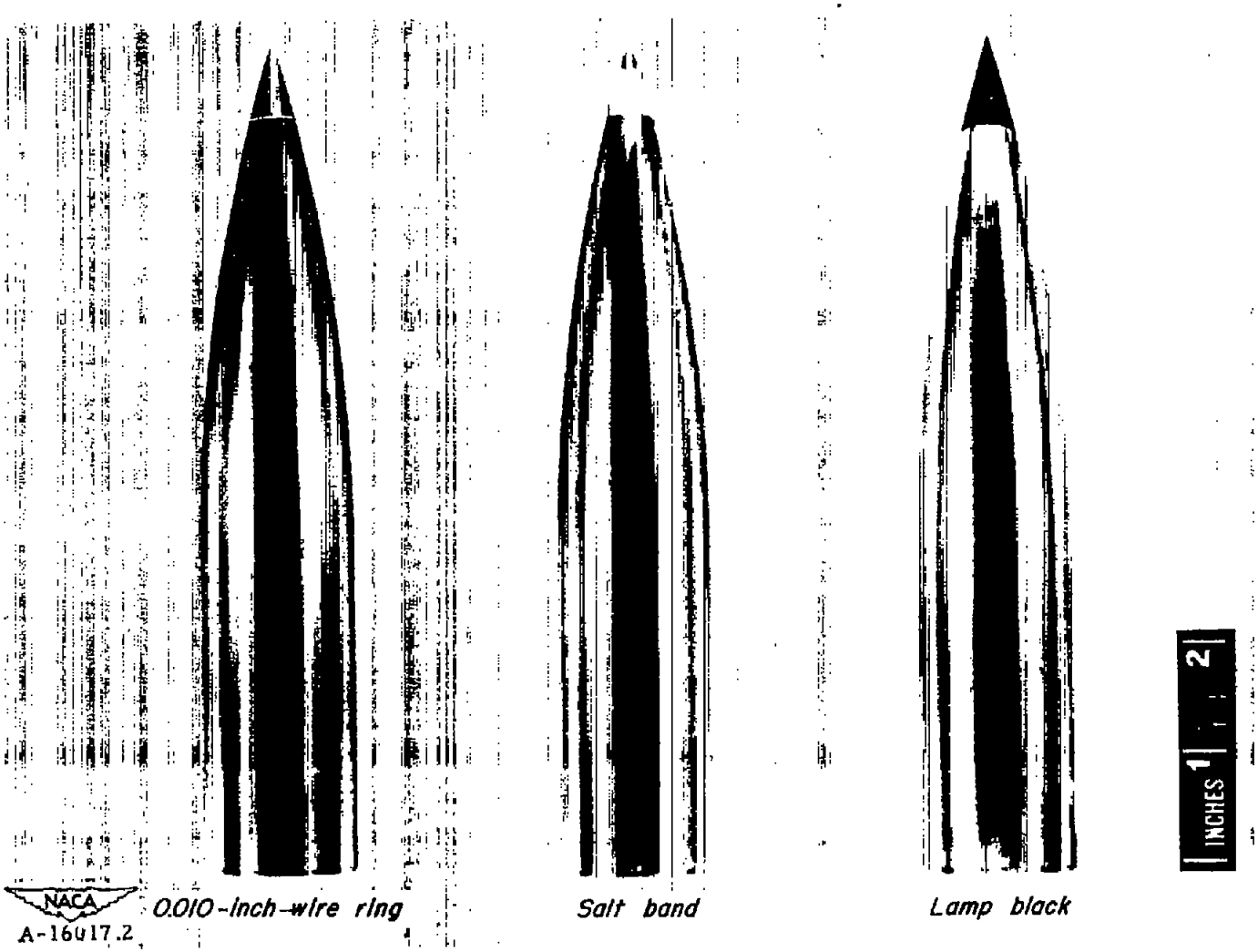

Figure 3.— Typical model with several boundary-layer-transition promoting devices.

(a) Laminar boundary layer.

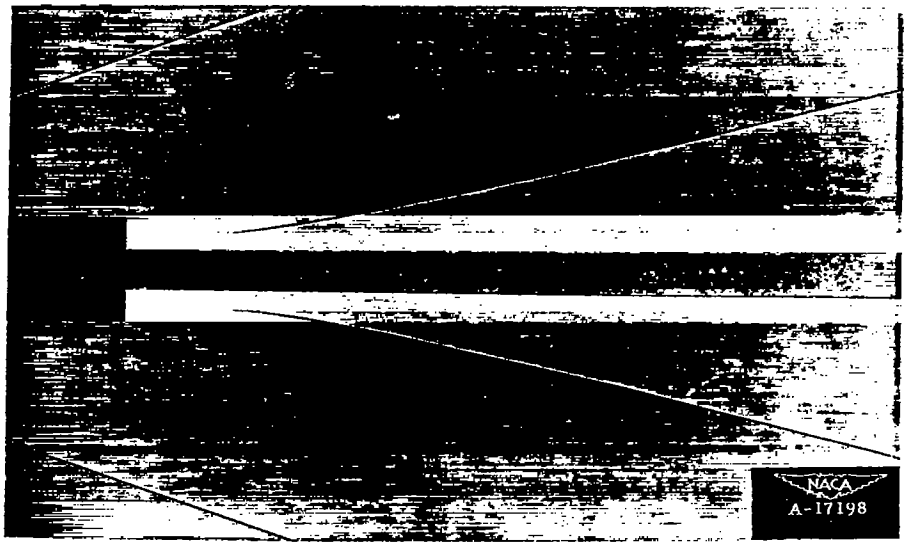

(b) Turbulent boundary layer, fixed transition.

Figure 4.— Shadowgraph pictures of flow around the base of a typical model; $M_o = 3.49$, $Re = 4.45 \times 10^6$.

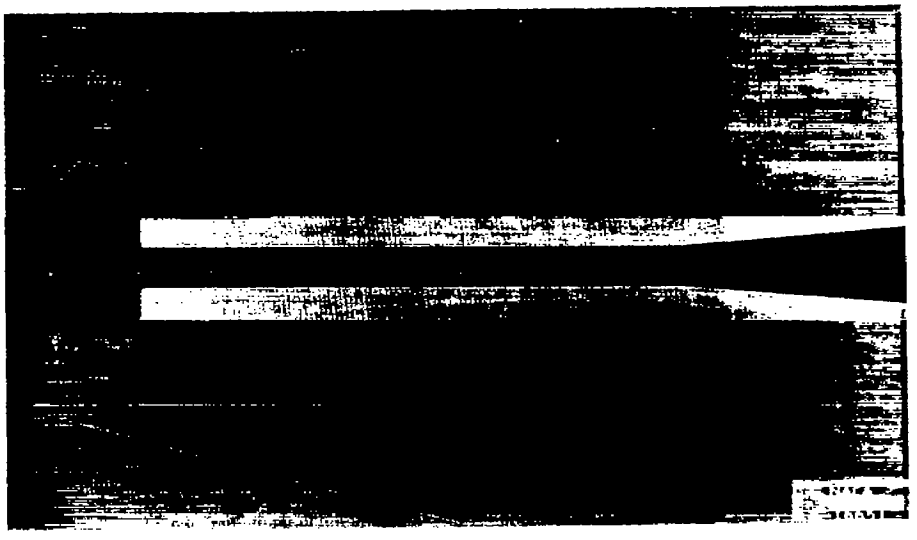

(c) Laminar boundary layer.

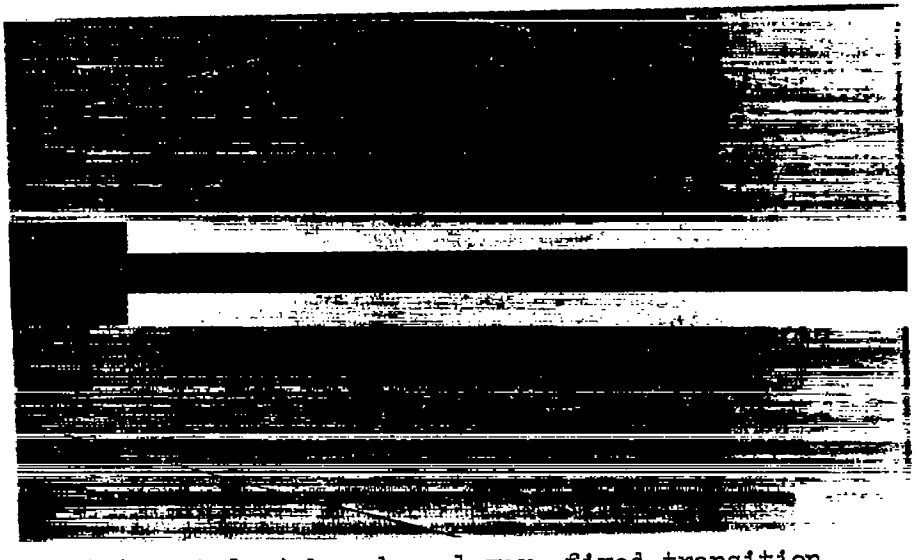

(d) Turbulent boundary layer, fixed transition.

Figure 4. – Concluded; $M_o = 4.48$, $Re = 1.75 \times 10^6$.

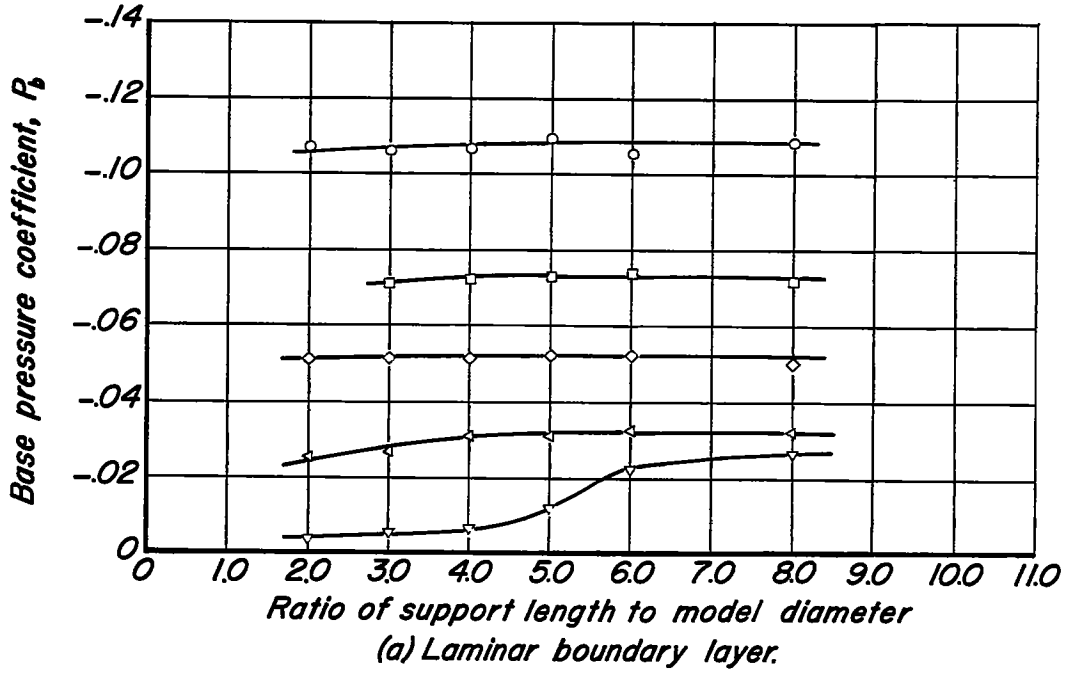

(a) Laminar boundary layer.

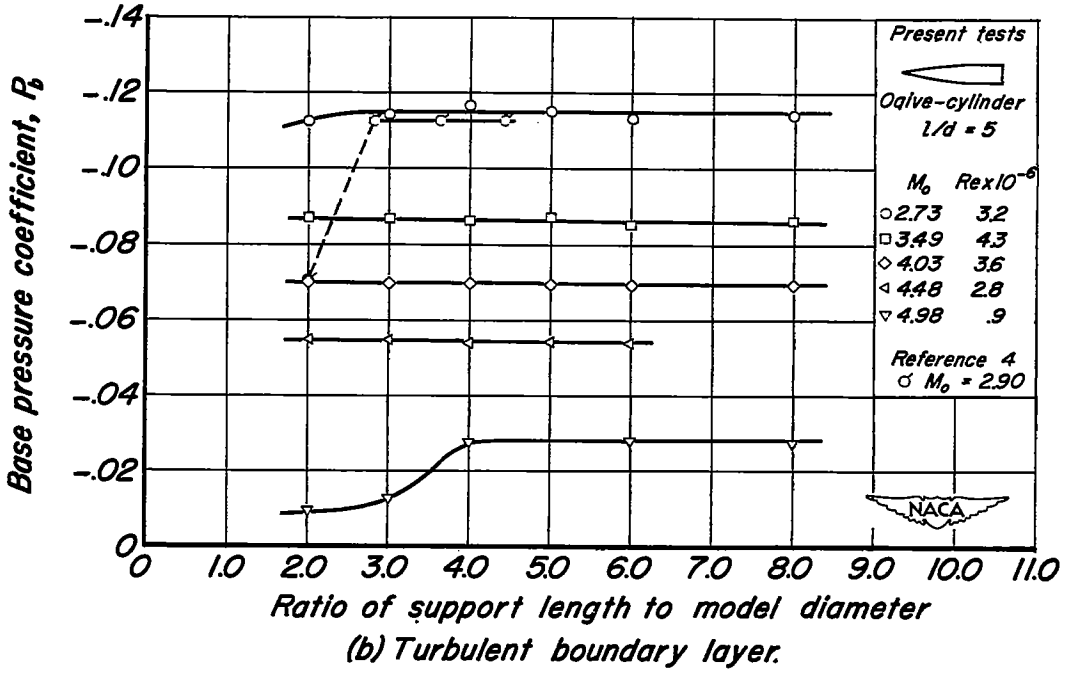

(b) Turbulent boundary layer.

Figure 5.–Effect of support length on base pressure; d_s/d= 0.375 (uncorrected for condensation).

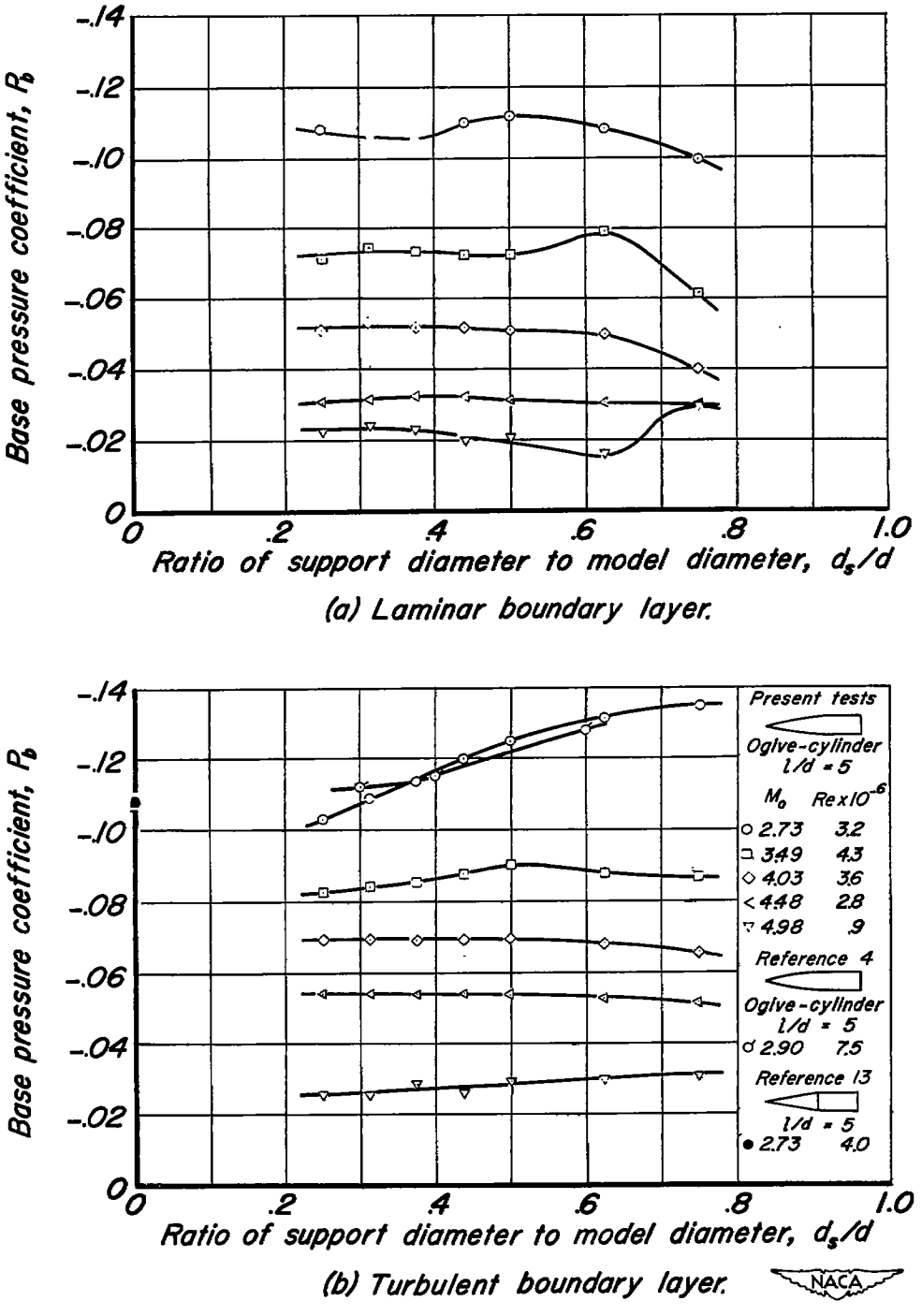

Figure 6.-Effect of support diameter on base pressure; $l_s/d = 6$ (uncorrected for condensation).

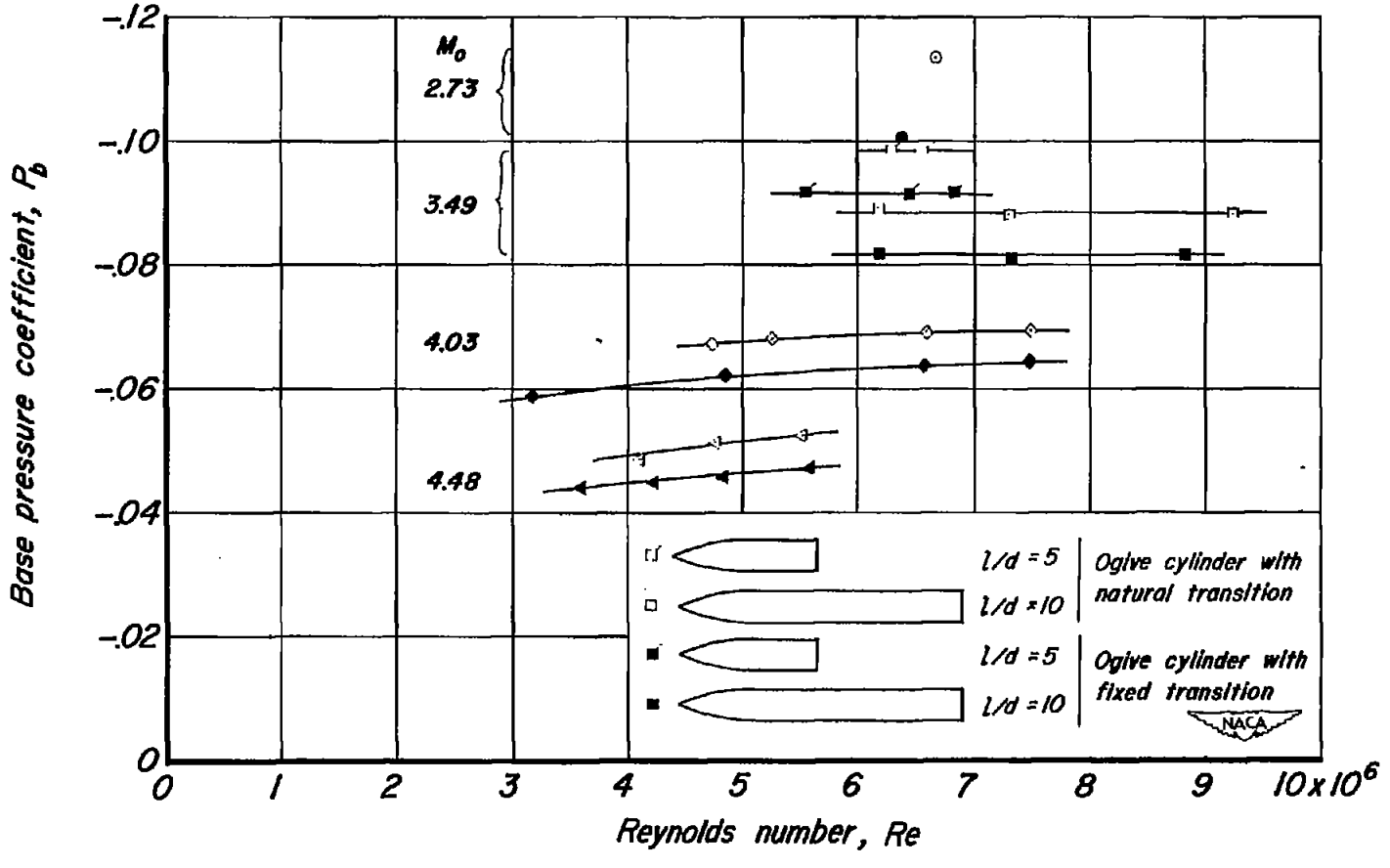

Figure 7.--Comparison of the base pressure with turbulent-boundary-layer flow for natural and artificially induced transition.

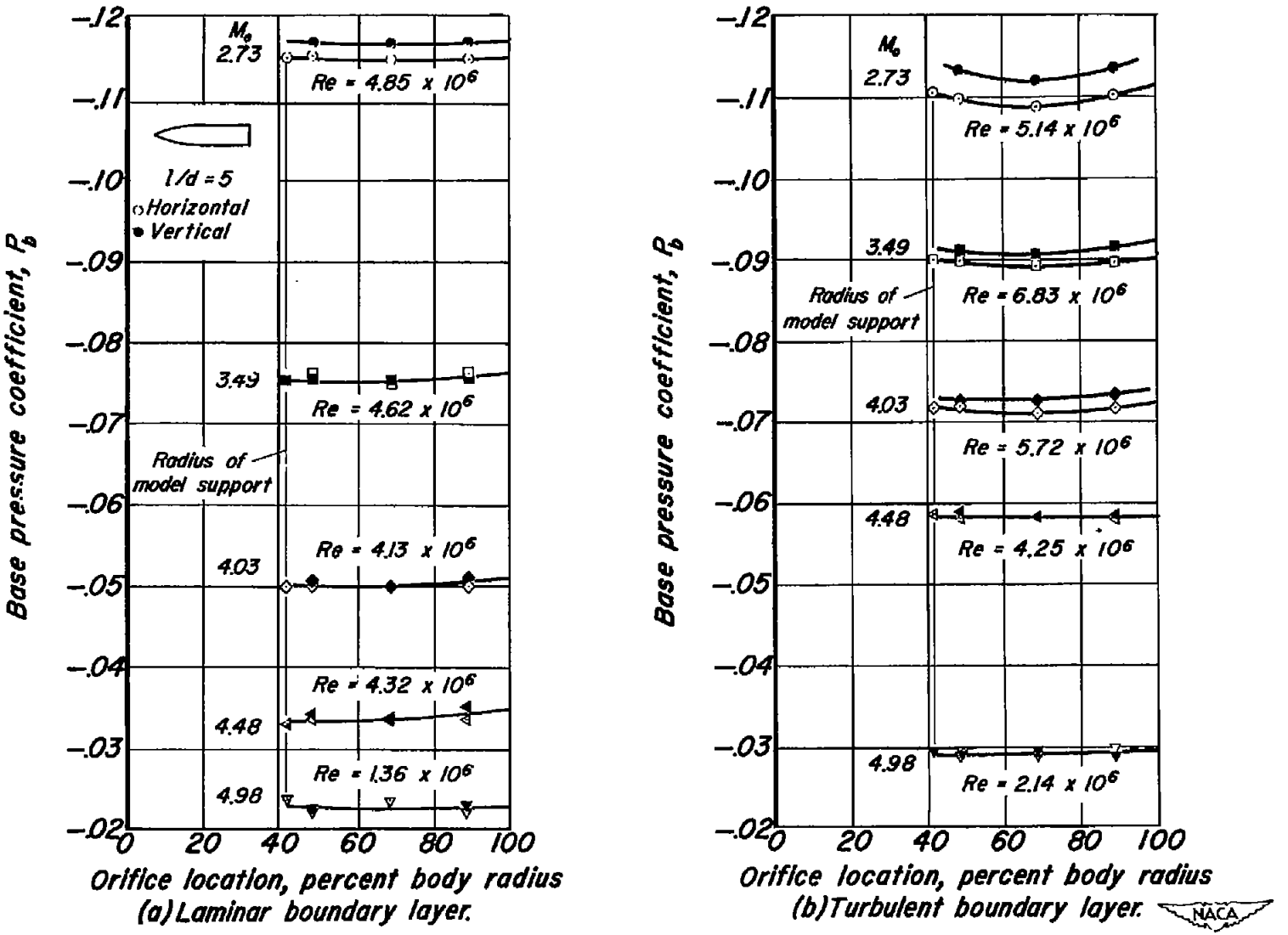

Figure 8.—Variation of base pressure coefficient with radial location (uncorrected for condensation).

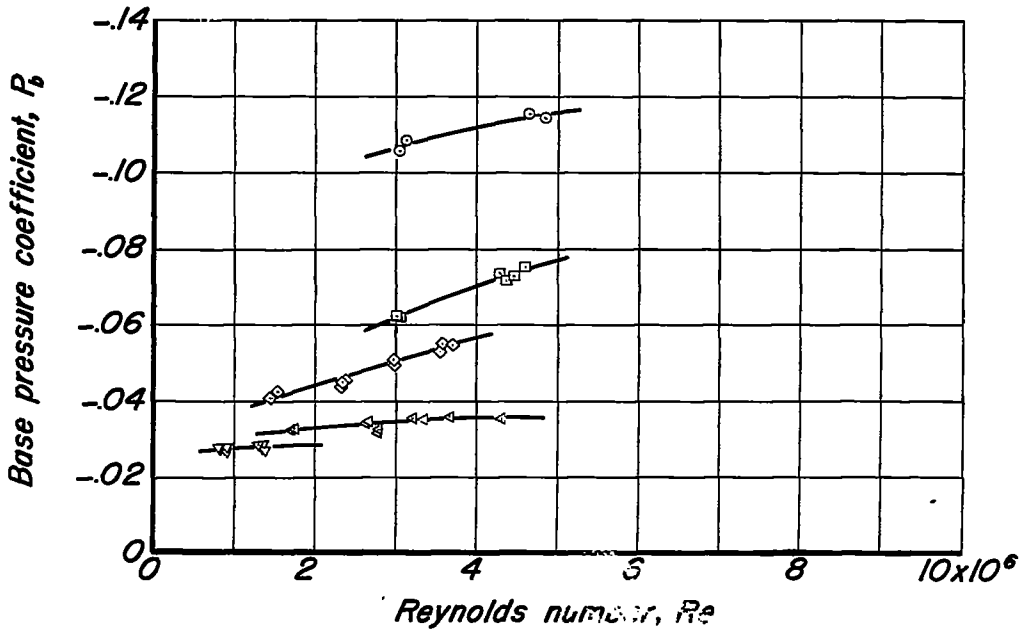

(a) Uncorrected for condensation.

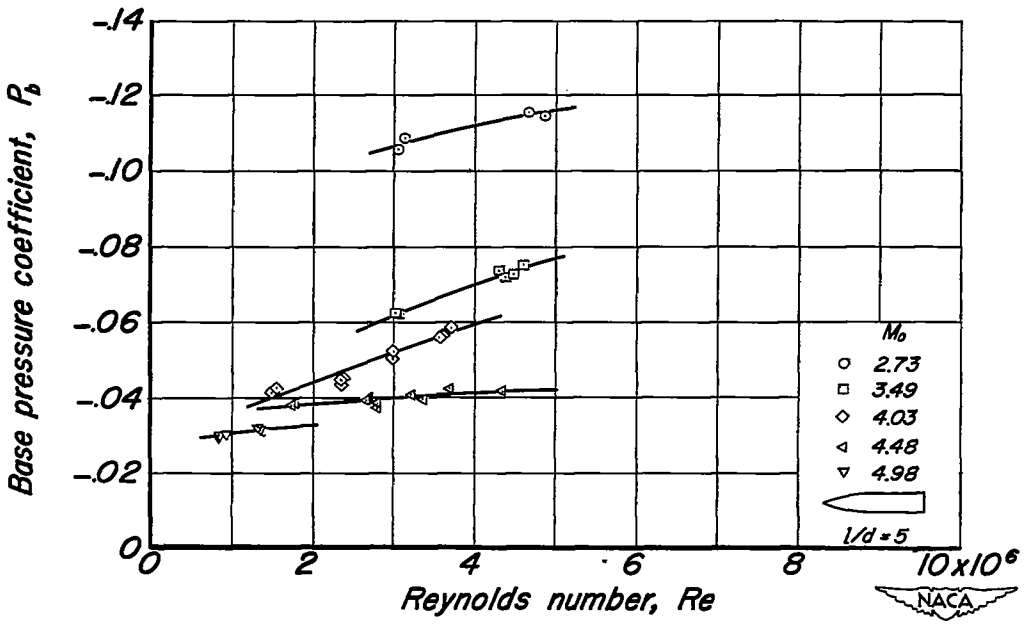

(b) Corrected for condensation.

Figure 9.—Variation of base pressure coefficient with Reynolds number at Mach numbers from 2.73 to 4.98 for laminar-boundary-layer flow.

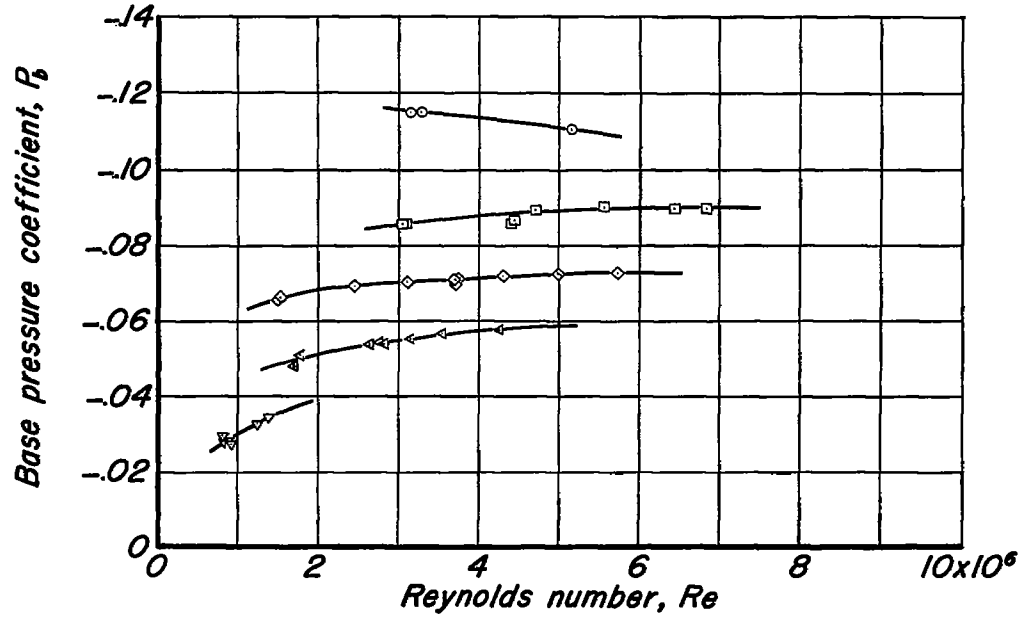

(a) Uncorrected for condensation.

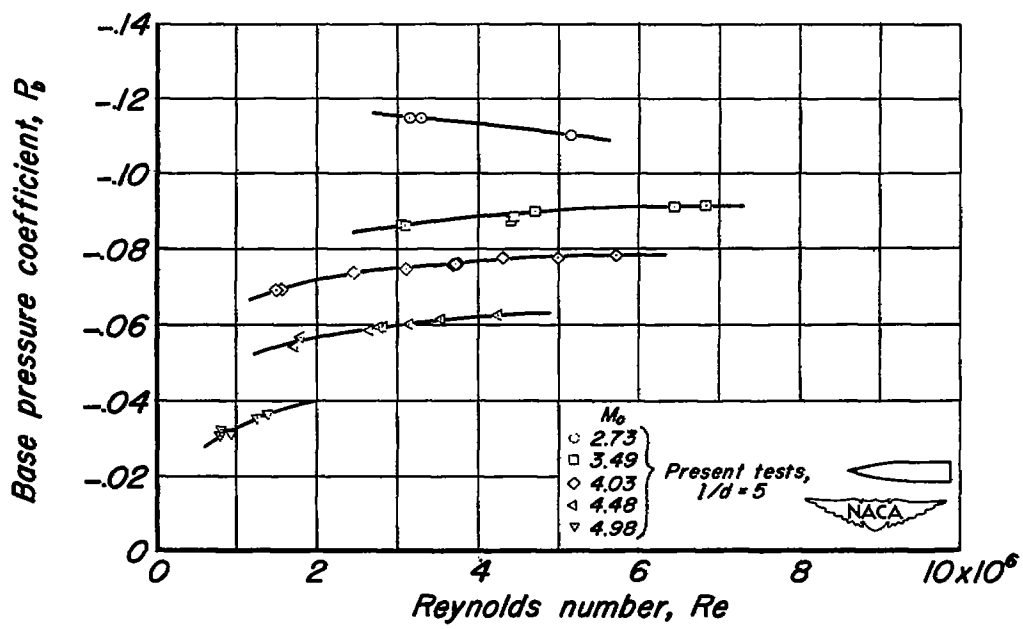

(b) Corrected for condensation.

Figure 10.–Variation of base pressure coefficient with Reynolds number at Mach numbers from 2.73 to 4.98 for turbulent-boundary-layer flow.

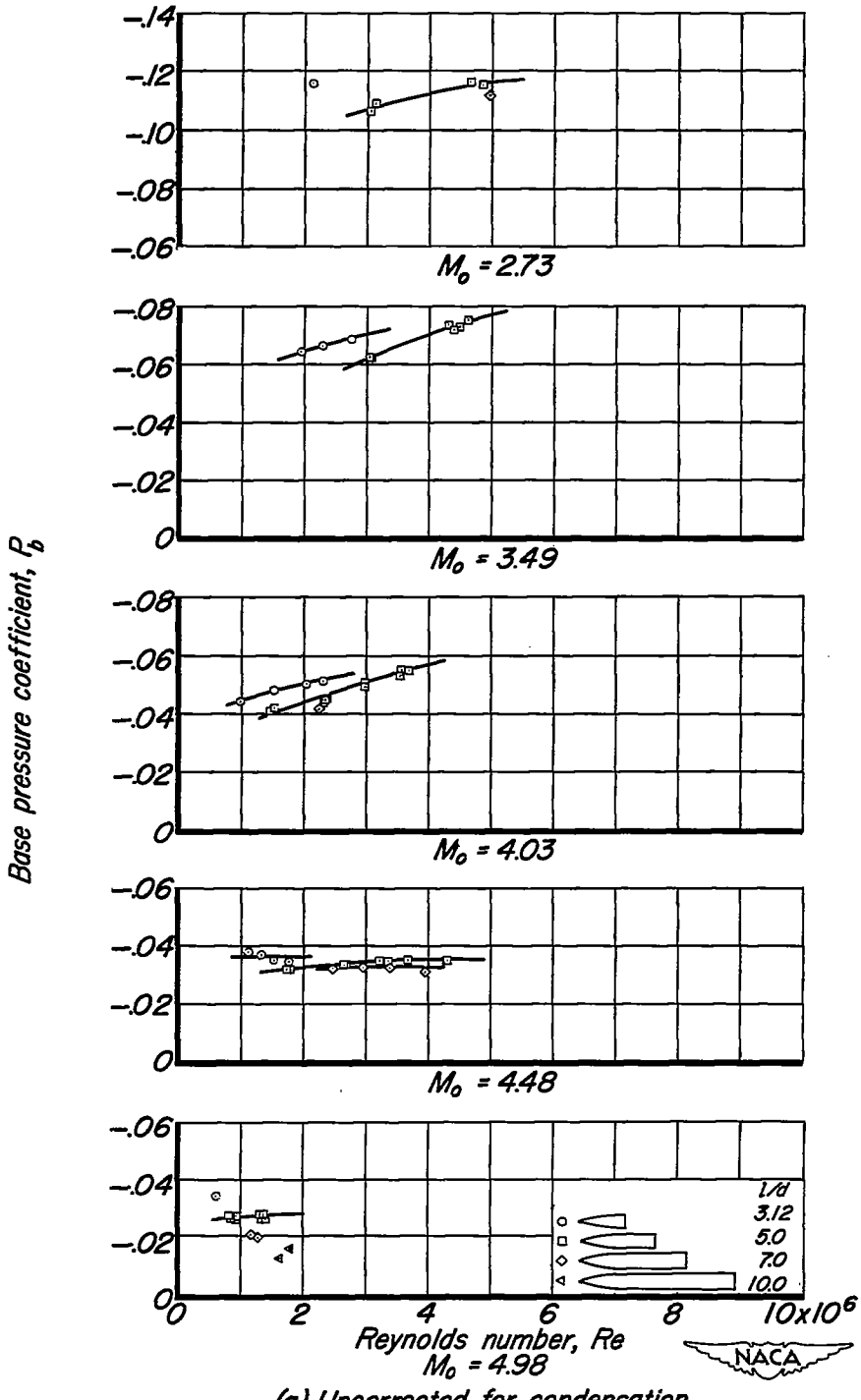

(a) Uncorrected for condensation.

Figure 11.-Variation of base pressure coefficient with Reynolds number for several fineness ratios; laminar-boundary-layer flow.

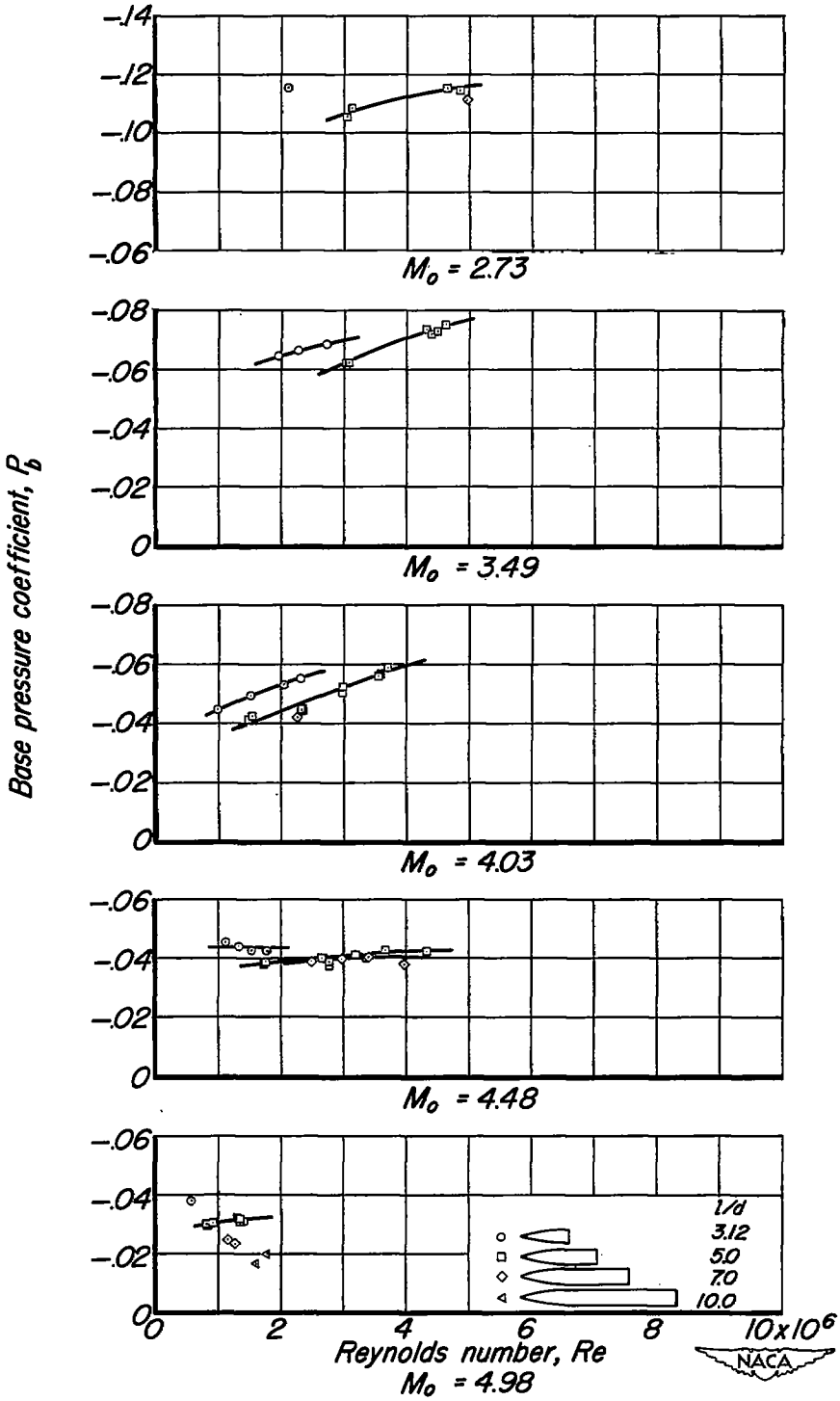

(b) Corrected for condensation.

Figure 11.—Concluded.

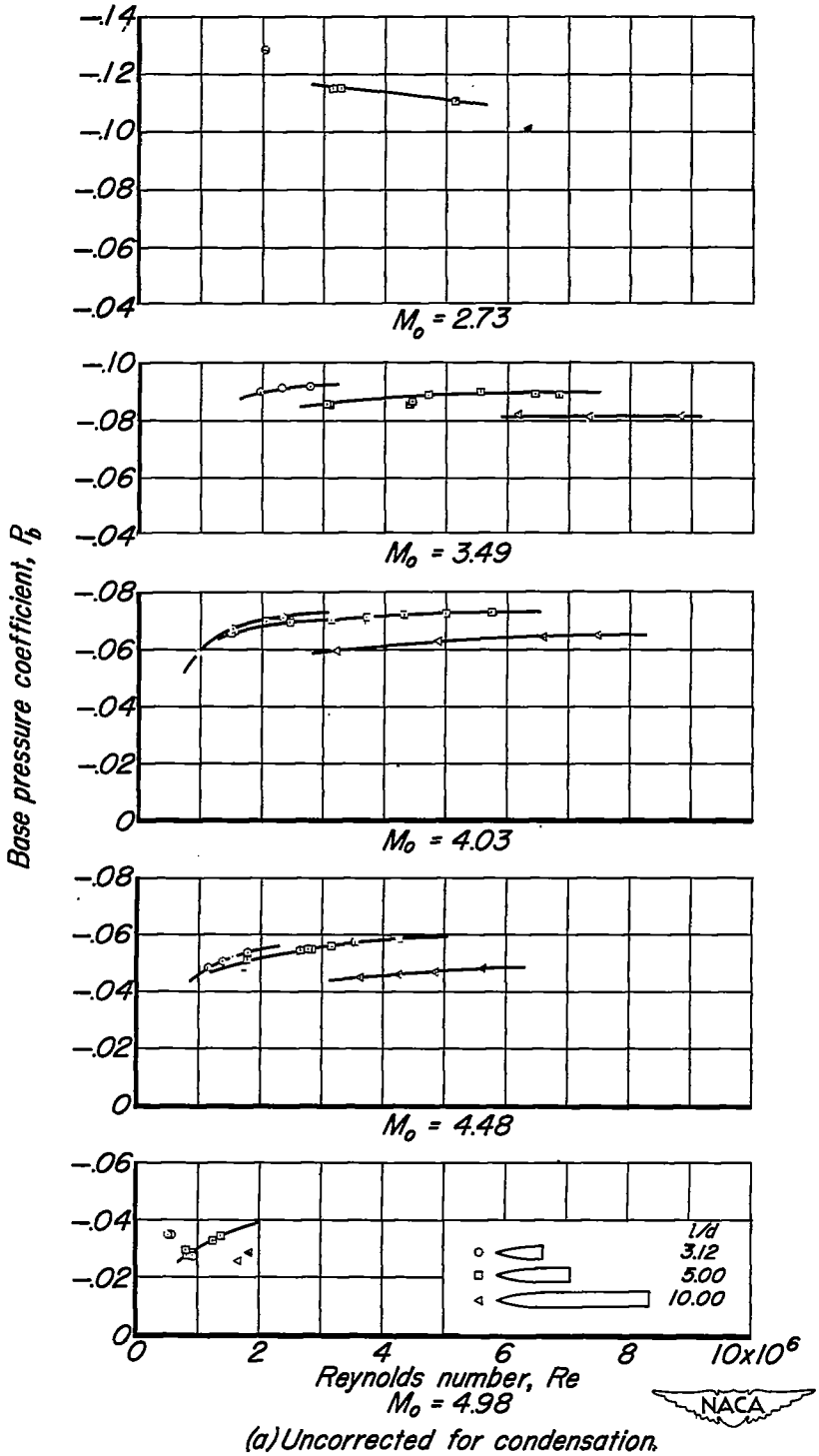

(a) Uncorrected for condensation.

Figure 12.-Variation of base pressure coefficient with Reynolds number for several fineness ratios; turbulent-boundary-layer flow.

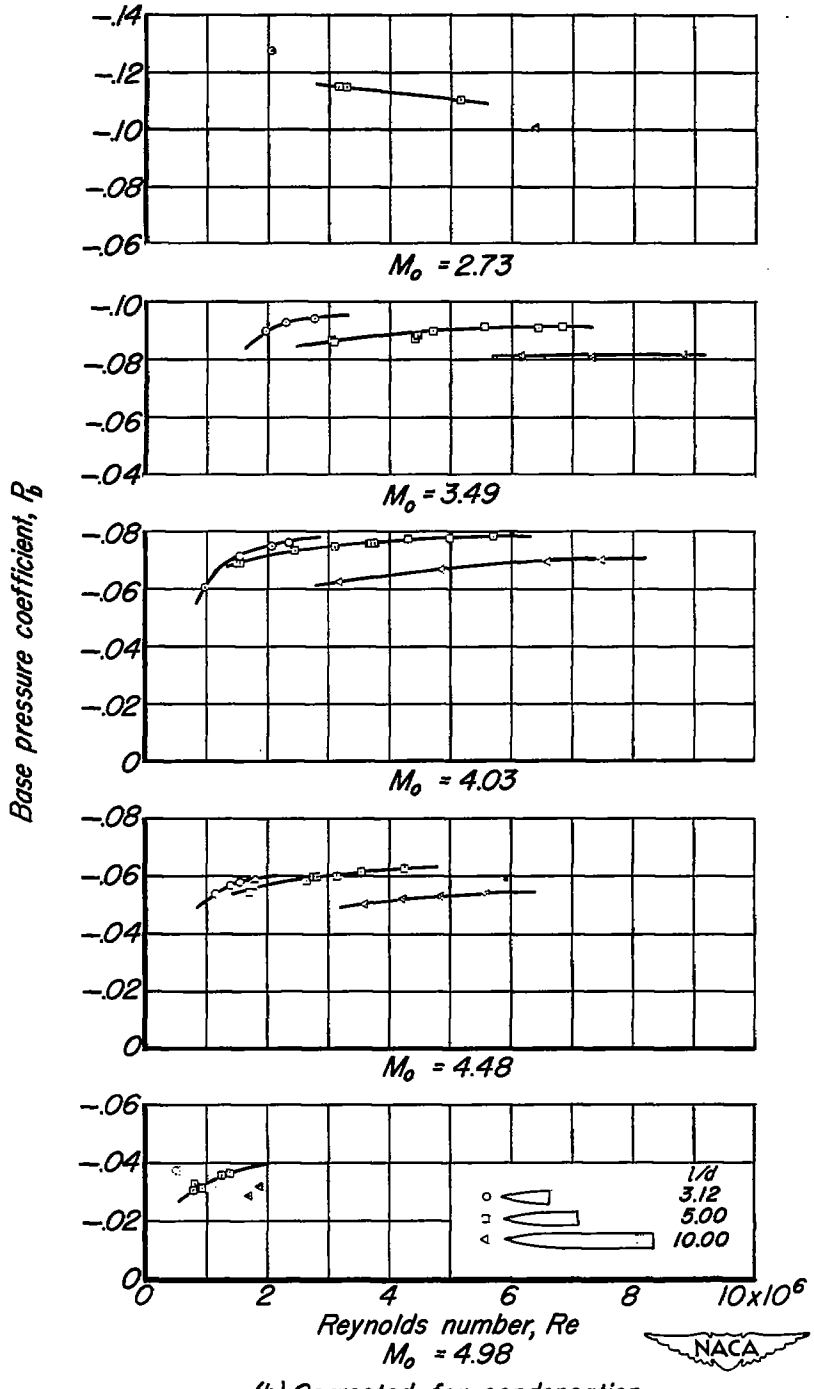

(b) Corrected for condensation.

Figure 12.– Concluded.

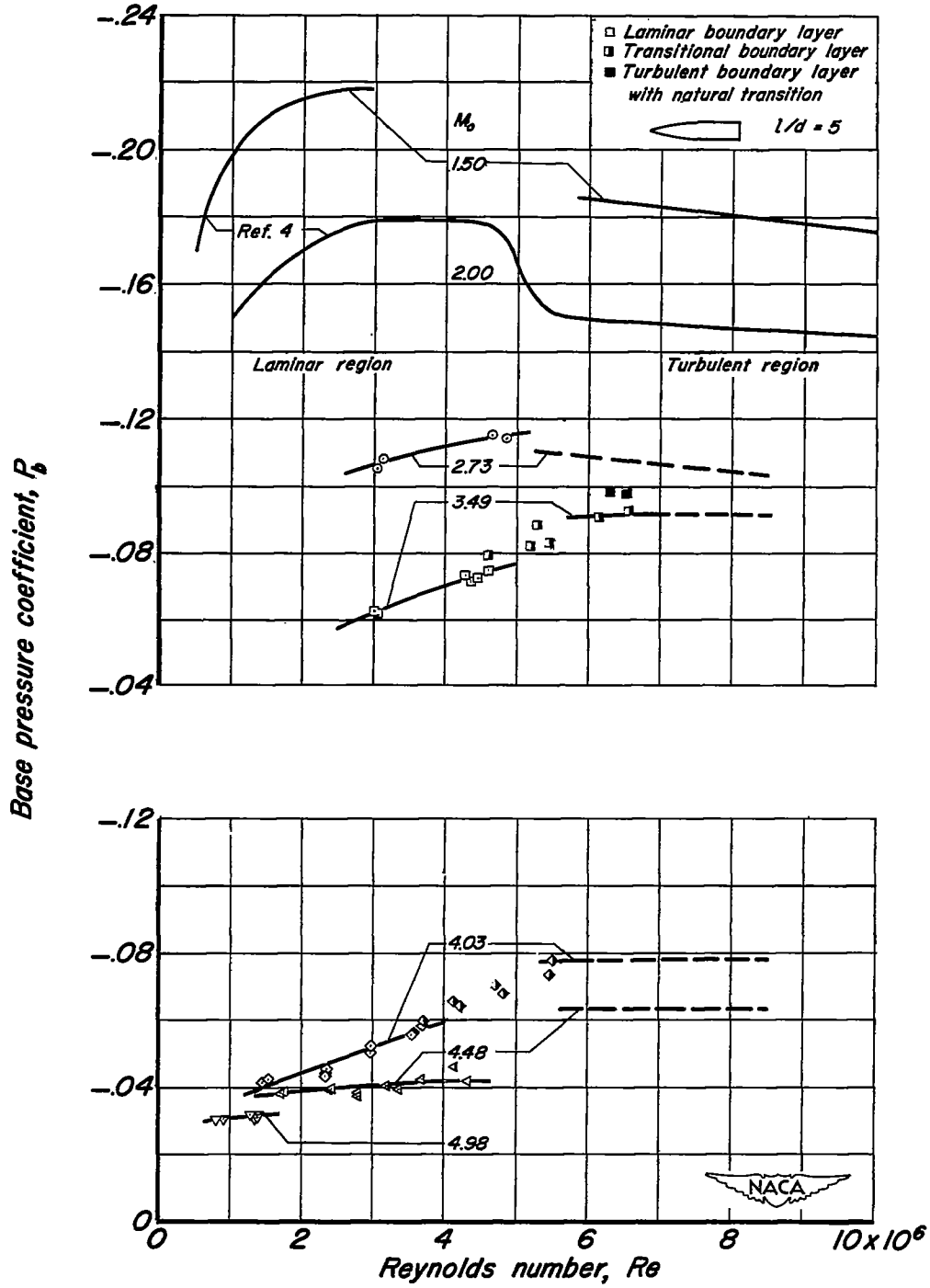

Figure 13.–Variation of base pressure coefficient with Reynolds number for different types of boundary layer flow (corrected for condensation).

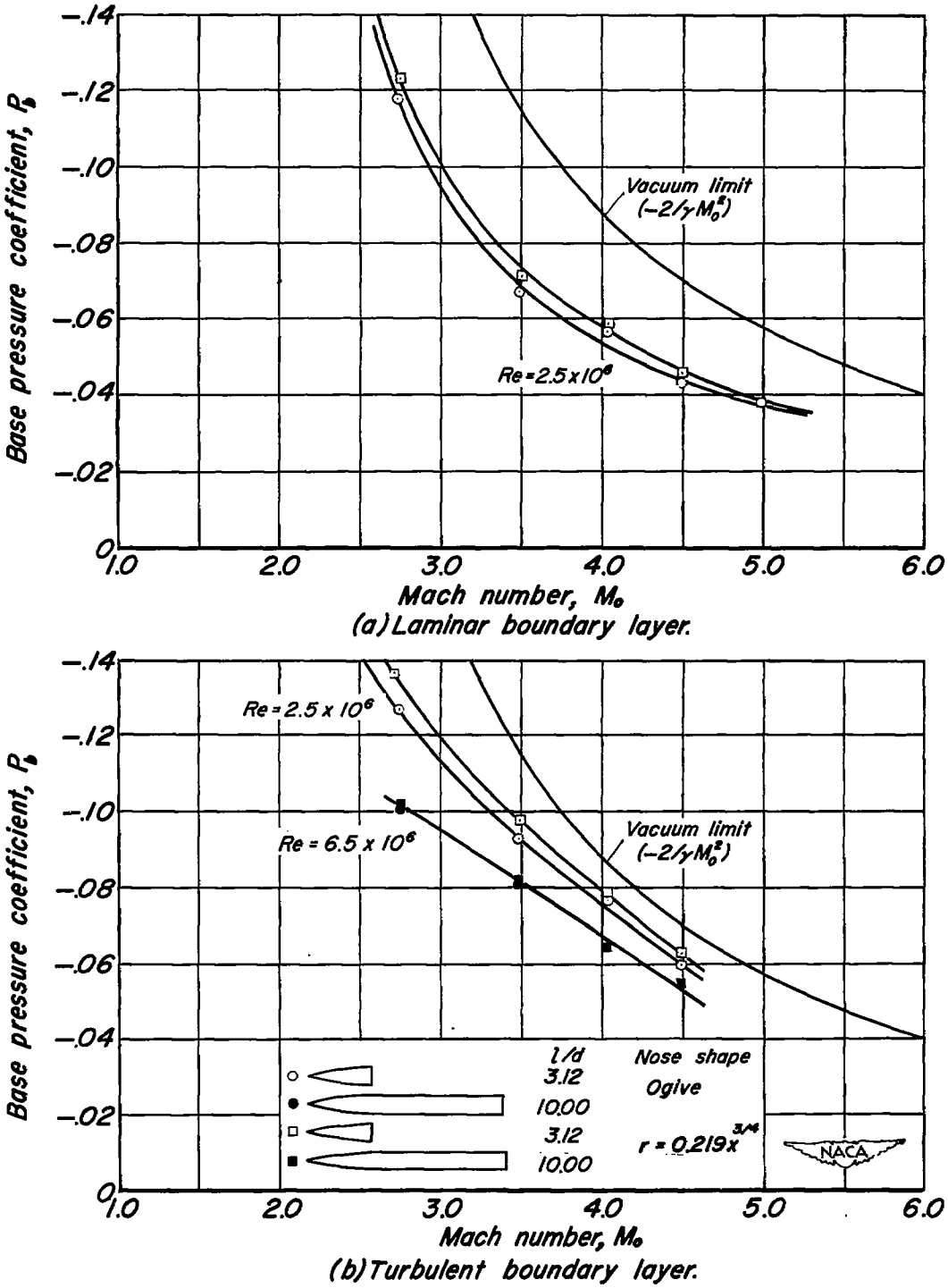

Figure 14.—Variation of base pressure coefficient with Mach number for several nose shapes (corrected for condensation).

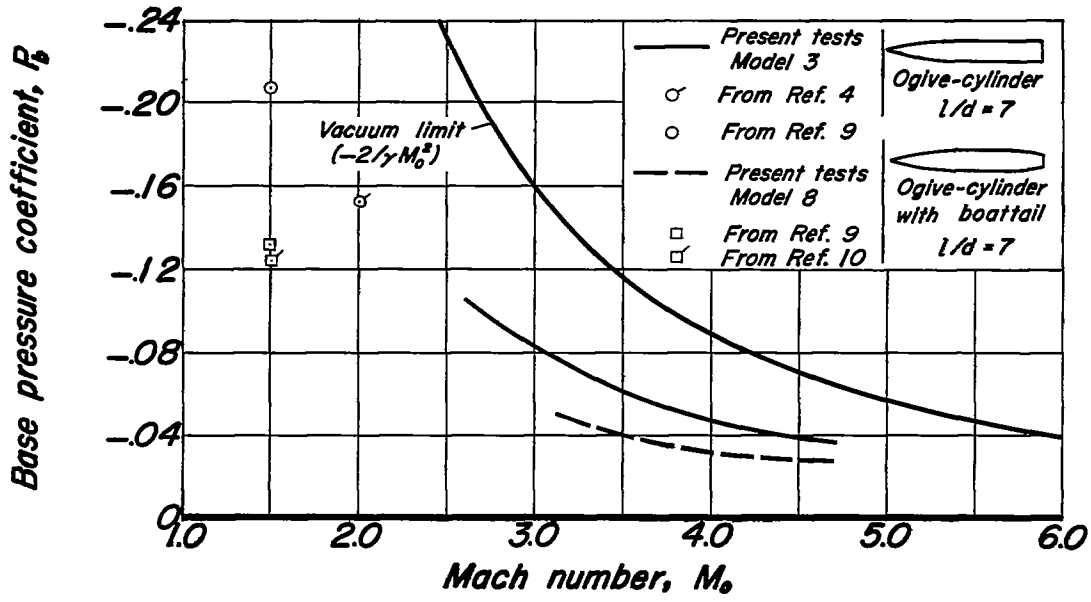

(a) Laminar boundary layer, $Re = 3.0 \times 10^6$

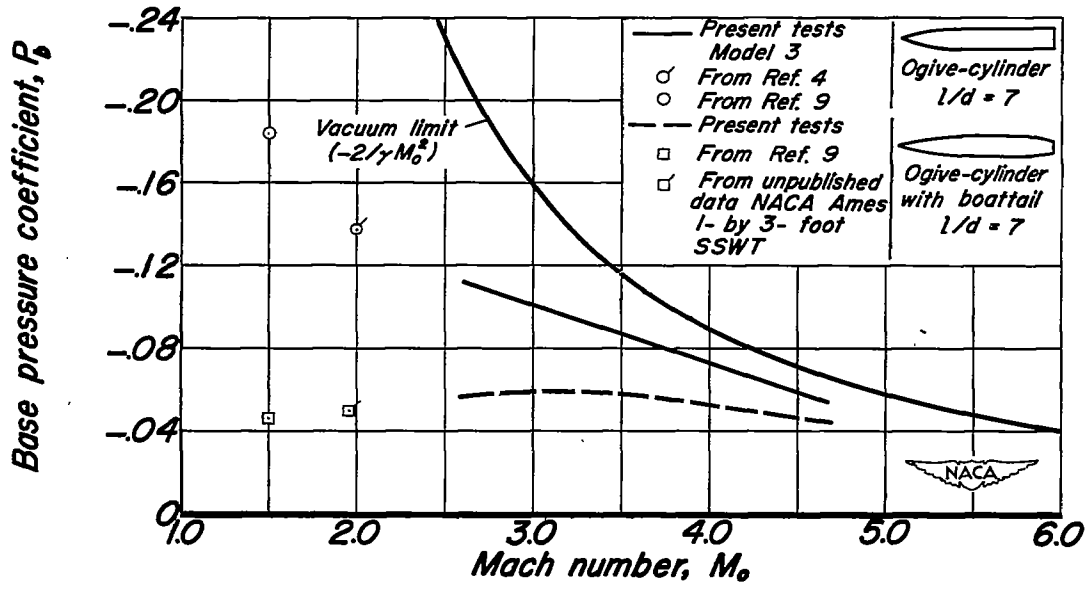

(b) Turbulent boundary layer, $Re = 5.0 \times 10^6$

Figure 15.–Comparison of base pressure coefficient with and without boattailing (corrected for condensation).

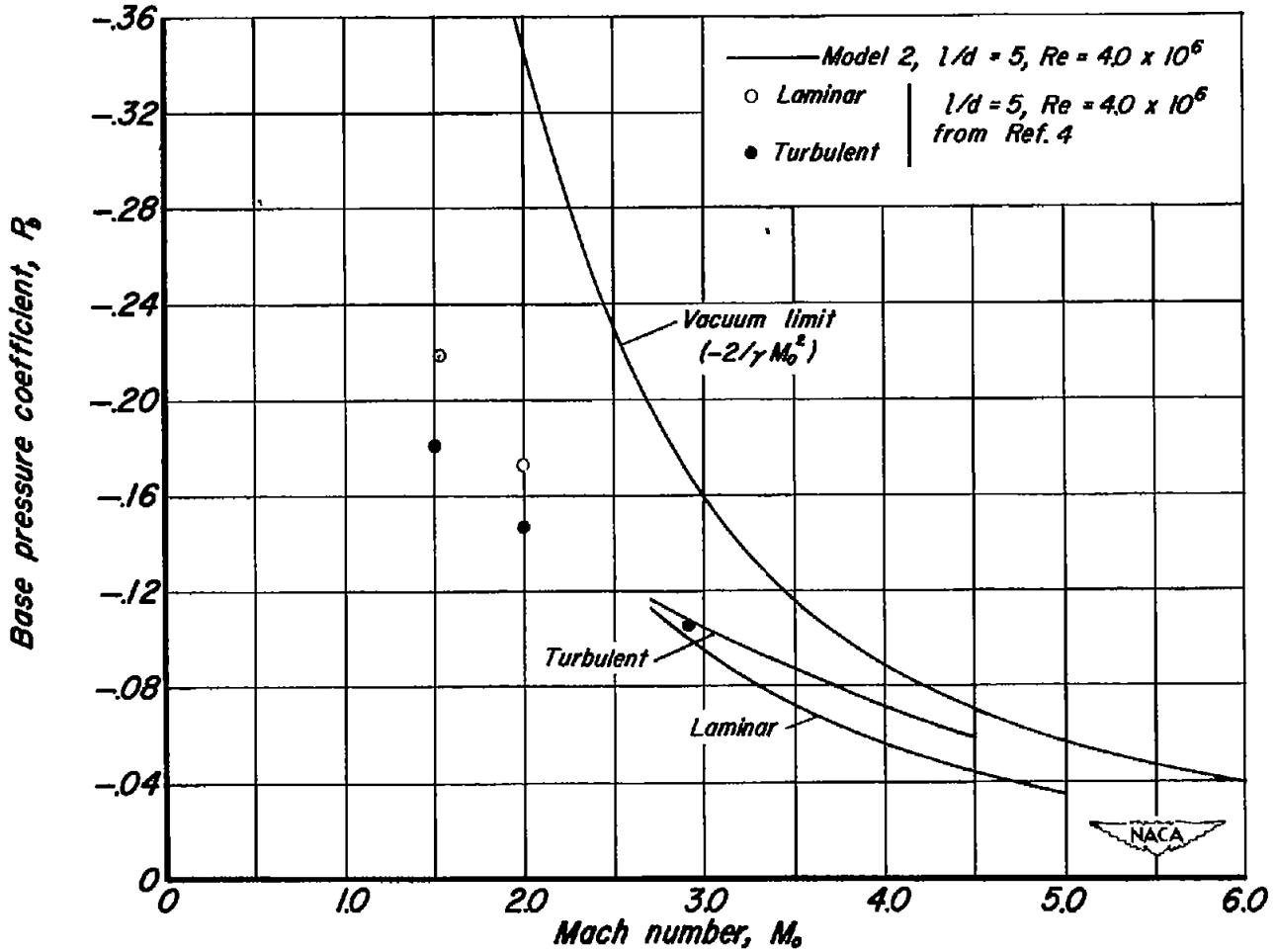

Figure 16.–Variation of base pressure coefficient with Mach number (corrected for condensation).

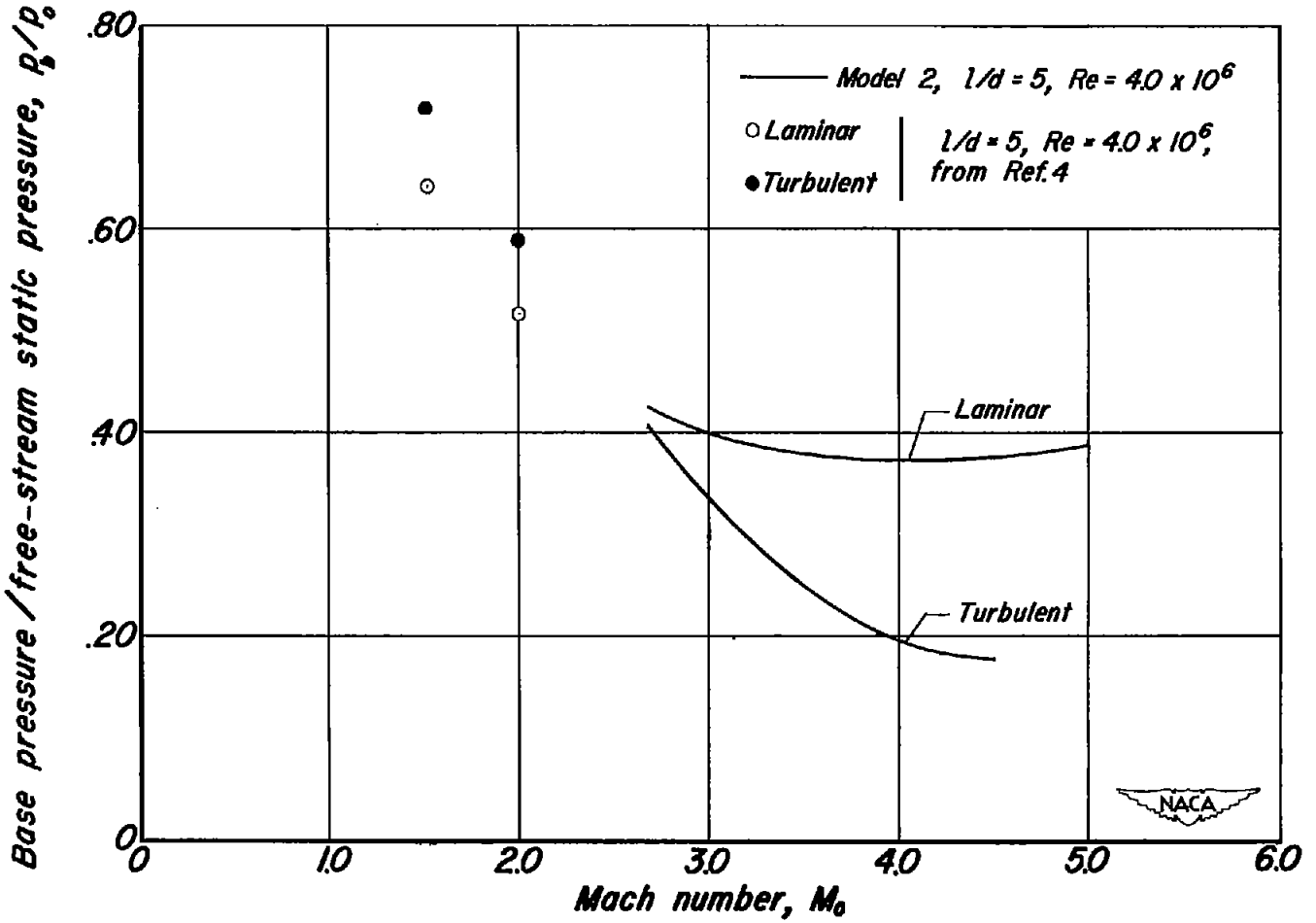

Figure 17.-Variation of the ratio of base pressure to free-stream static pressure (p_b/p_o) with Mach number (corrected for condensation).

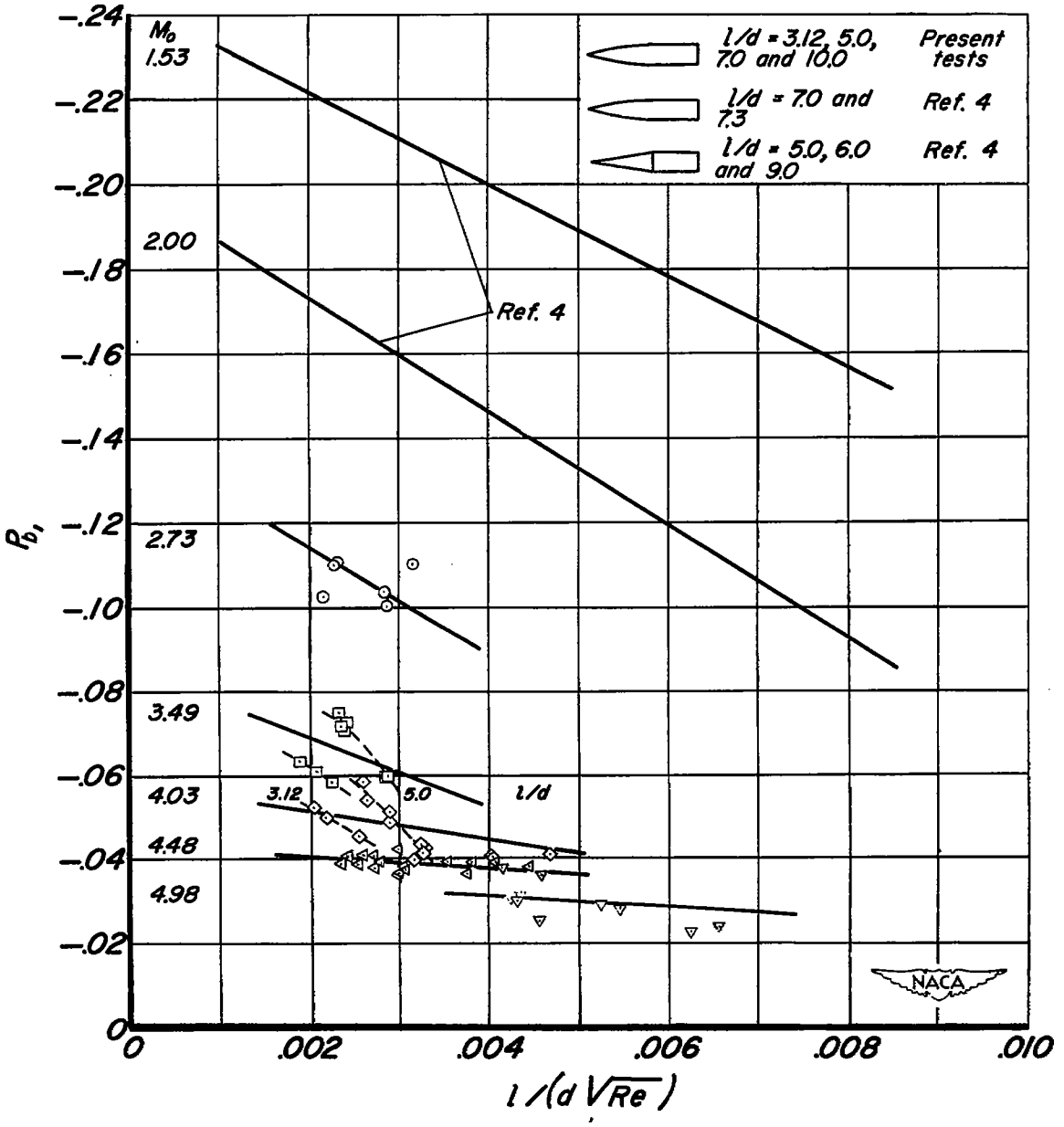

(a) Laminar boundary layer.

Figure 18.—Base pressure data correlation (corrected for condensation).

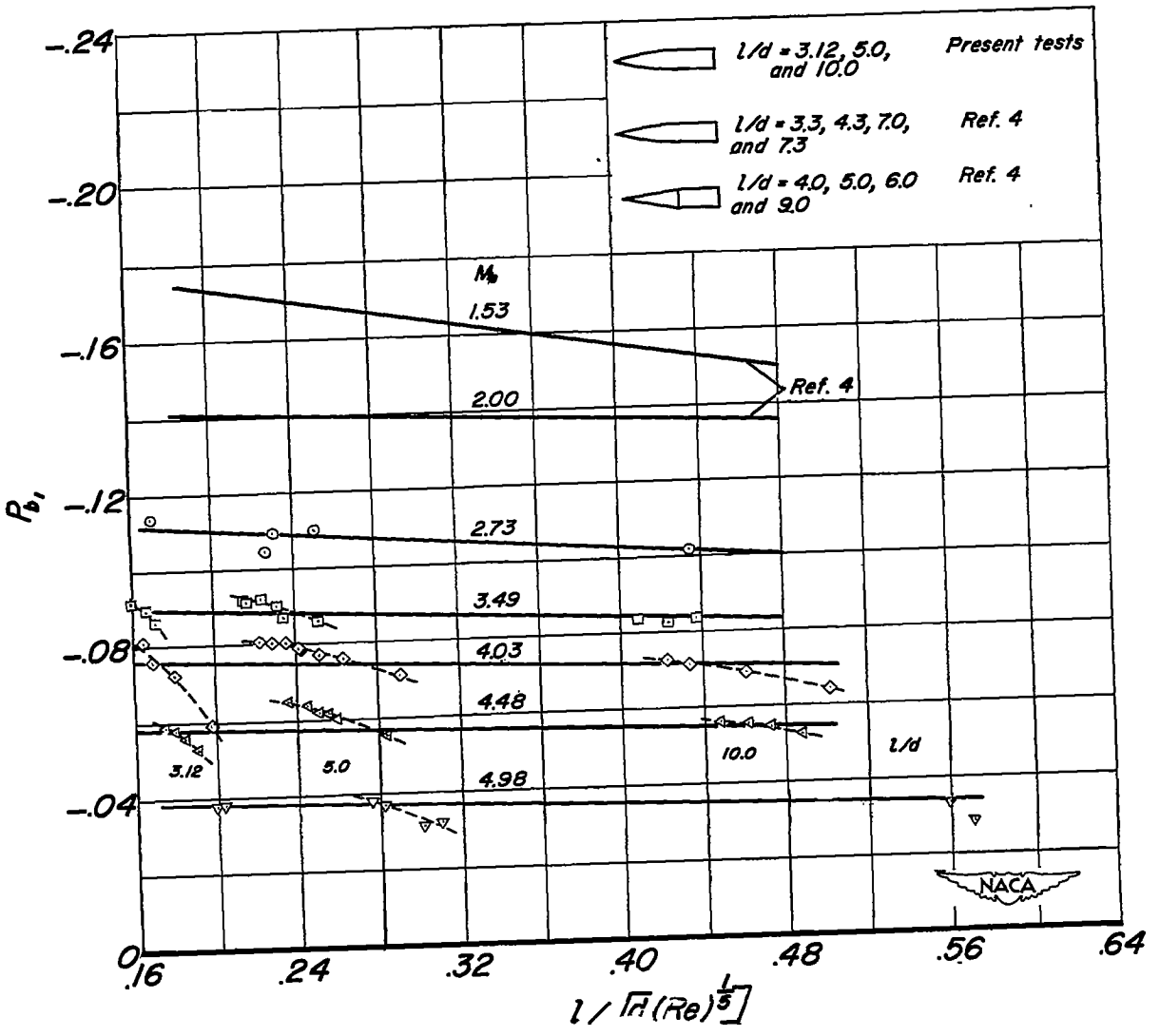

(b) Turbulent boundary layer.

Figure 18.—Concluded.